Review of *Orthochiroides* Kovařík, 1998 with description of a new species (Scorpiones: Buthidae)

František Kovařík & Graeme Lowe

Euscorpius is the first research publication completely devoted to scorpions (Arachnida: Scorpiones). *Euscorpius* takes advantage of the rapidly evolving medium of quick online publication, at the same time maintaining high research standards for the burgeoning field of scorpion science (scorpiology). *Euscorpius* is an expedient and viable medium for the publication of serious papers in scorpiology, including (but not limited to): systematics, evolution, ecology, biogeography, and general biology of scorpions. Review papers, descriptions of new taxa, faunistic surveys, lists of museum collections, and book reviews are welcome.

Derivatio Nominis

The name *Euscorpius* Thorell, 1876 refers to the most common genus of scorpions in the Mediterranean region and southern Europe (family Euscorpiidae).

Euscorpius is located at: https://mds.marshall.edu/euscorpius/
Archive of issues 1-270 see also at: http://www.science.marshall.edu/fet/Euscorpius

(Marshall University, Huntington, West Virginia 25755-2510, USA)

ICZN COMPLIANCE OF ELECTRONIC PUBLICATIONS:

Electronic ("e-only") publications are fully compliant with ICZN (*International Code of Zoological Nomenclature*) (i.e. for the purposes of new names and new nomenclatural acts) when properly archived and registered. All *Euscorpius* issues starting from No. 156 (2013) are archived in two electronic archives:

- **Biotaxa,** http://biotaxa.org/Euscorpius (ICZN-approved and ZooBank-enabled)
- **Marshall Digital Scholar**, http://mds.marshall.edu/euscorpius/. (This website also archives all *Euscorpius* issues previously published on CD-ROMs.)

Between 2000 and 2013, ICZN **did not accept online texts** as "published work" (Article 9.8). At this time, *Euscorpius* was produced in two **identical** versions: online (*ISSN 1536-9307*) and CD-ROM (*ISSN 1536-9293*) (laser disk) in archive-quality, read-only format. Both versions had the identical date of publication, as well as identical page and figure numbers. **Only copies distributed on a CD-ROM** from *Euscorpius* in 2001-2012 represent published work in compliance with the ICZN, i.e. for the purposes of new names and new nomenclatural acts.

In September 2012, ICZN Article 8. What constitutes published work**,** has been amended and allowed for electronic publications, disallowing publication on optical discs. From January 2013, *Euscorpius* discontinued CD-ROM production; only online electronic version (ISSN 1536-9307) is published. For further details on the new ICZN amendment, see http://www.pensoft.net/journals/zookeys/article/3944/.

Review of *Orthochiroides* Kovařík, 1998
with description of a new species (Scorpiones: Buthidae)

František Kovařík & Graeme Lowe

[1] P. O. Box 27, CZ-145 01 Praha 45, Czech Republic; http://www.scorpio.cz
[2] Monell Chemical Senses Center, 3500 Market St., Philadelphia, PA 19104-3308, USA

Summary

The genus *Orthochiroides* Kovařík, 1998 is reanalyzed. Revised diagnoses and new illustrations for the genus and all four of its species are presented. A new species, *O. somalilandus* **sp**. **n**. from Somaliland is described and illustrated. Phylogenetic relationships of the genus with several other similar genera of small buthids are inferred from a parsimony analysis of 43 discrete morphological characters. The recent synonymy of *Orthochiroides* with *Orthochirus* is refuted and the genus is revalidated.

Introduction

In 1899, Pocock described *Butheolus insularis*, a small, dark scorpion from Socotra Island (Yemen) with a trapezoidal carapace, short pedipalps and incrassate, heavily sclerotized posterior metasomal segments IV–V. The lateral and ventral surfaces of those segments were smooth, and were marked with numerous small, shallow depressions or punctae. The punctate metasoma differed from that of the type species of the genus, *Butheolus thalassinus* Simon, 1882, in which the posterior metasomal segments are granulate and non-punctate. However, it was similar to that of *B*. *aristidus* Simon, 1992, originally also described under the same genus. Subsequently, Simon (1910) transferred *B*. *aristidus* to *Orthochirus* Karsch, 1891, a genus characterized by smooth, punctate metasomal segments. Birula (1917) listed under *Orthochirus* several other species with punctate metasomal segments that were previously assigned to *Butheolus*, including *B*. *insularis*. Levy & Amitai (1980), in a checklist, downgraded *Orthochirus insularis* to a subspecies of *Orthochirus bicolor* (Pocock, 1897), without explanation.

Kovařík (1998) described the monotypic genus *Orthochiroides*, with type species *Orthochiroides vachoni* from Somalia. The species was named after Max Vachon, who in 1976 examined all 38 type specimens (VA No. 1405). Vachon sorted the material into males, females and juveniles, and attached to it the label "*Orthochiroides* gen. nov.", a name that he never published. *Orthochiroides vachoni* is a small, dark scorpion, superficially resembling *Orthochirus* in habitus, but differing in at least two characters: the shape of the telson vesicle is bulbous in *O*. *vachoni*, vs. slender and pyriform in *Orthochirus*; and the morphosculpture of the lateral and ventral surfaces of metasoma IV–V is rugose-reticulate with large depressions in *O*. *vachoni*, vs. smooth with

small punctae in *Orthochirus*. Subsequently, Kovařík (2004) revised *Orthochiroides*, expanding it to include *Butheolus insularis*, and described a second species from Socotra Island, *O*. *socotrensis*. The two Socotra species both bear smooth, punctate metasomal segments, a surface morphosculpture similar to that of *Orthochirus*. This left the shape of the telson as the main diagnostic character for separating the two genera. Recently, the genus *Orthochiroides* was rejected by Lourenço & Ythier (2021). After studying a paratype male of *Orthochiroides vachoni* deposited in the Paris museum (MNHN), these authors concluded that telson shape was not a valid generic character, that no other differences from *Orthochirus* justified generic status, and hence that *Orthochiroides* Kovařík, 1998, was a junior synonym of *Orthochirus* Karsch, 1891. Here, we revisit the question about the validity of the genus *Orthochiroides*. We analyze in detail the morphology of the species previously assigned to *Orthochiroides*. We compare them to species described under *Orthochirus*, and several other genera of small buthids that share a number of characters with *Orthochirus*. Our results support the reinstatement of *Orthochiroides*. We also describe a new species of *Orthochiroides*.

Methods, Material & Abbreviations

Nomenclature and measurements generally follow Stahnke (1971), Sissom et al. (1990), Kovařík (2009), Kovařík & Ojanguren Affilastro (2013) and Lowe et al. (2014). Nomenclature of trichobothria largely follows Vachon (1974, 1975), of hemispermatophores Kovařík et al. (2018), and of pedipalp chela carination, Acosta et al. (2008). External morphology was examined under a dissecting microscope, viewing reflected white light or fluorescence emission under UV LED illumination. Hemispermatophore capsules were

imaged with a Mitutoyo M Plan Apo 10X objective. Focus stacking was implemented in Zerene Stacker 1.04 (Zerene Systems, LLC). Biometrics were measured with an ocular reticule or by digital image analysis with ImageJ 1.52a (Rasband, 2018). Cladistic analyses were conducted in TNT 1.5 (Goloboff & Catalano, 2016). Heuristic searches were performed by generating 1,000 random addition sequences with tree-bisection-reconnection (TBR) branch swapping, holding 50 trees per replicate. Trees were collapsed during searches with minimum length zero. Searches were performed under equal weights (EW), and under implied weights (IW) (Goloboff, 1993) testing a range of concavity constants. Unambiguous synapomorphies were mapped in TNT to the most parsimonious trees (MPTs) retrieved. Consistency indices (CI) and retention indices (RI) of trees and characters were calculated using scripts "stats.run" and "wstats.run". Node supports and average tree supports were estimated by jackknife resampling (4,000 pseudoreplicates, probability 36%) expressed as group present/ contradicted (GC) frequency differences (Goloboff et al., 2003). Absolute or relative Bremer supports were also estimated, using up to 40,000 suboptimal trees generated by successive TBR branch swapping of MPTs and increasingly suboptimal trees. *Specimen depositories*: BMNH (The Natural History Museum, London, United Kingdom); FKCP (František Kovařík, private collection, Prague, Czech Republic; will in future be merged with the collections of the National Museum of Natural History, Prague, Czech Republic); GLPC (Graeme Lowe, private collection, Auckland, New Zealand), MNHN (Muséum National d'Histoire Naturelle, Paris, France); MNHW (Museum of Natural History Wrocław, Wrocław, Poland); MZUF (Museo Zoologico de "La Specola", Firenze, Italy); NHMB (Naturhistorisches Museum, Basel, Switzerland); NMPC (National Museum of Natural History, Prague, Czech Republic); NMK (National Museums of Kenya, Nairobi, Kenya); ONHM (Oman Natural History Museum, Muscat, Oman); USNM (United States National Museum of Natural History (Smithsonian Institution), Washington, DC, USA); ZMHB (Museum für Naturkunde der Humboldt-Universität, Berlin, Germany); WDS (W. David Sissom, private collection, Canyon, Texas, USA); and ZMUH (Centrum für Naturkunde (CeNak), Center of Natural History Universität Hamburg, Zoological Museum, Hamburg, Germany). *Abbreviations*: morphometrics: D, depth; L, length; W, width; movable finger dentition: ID, inner denticles; OD, outer denticles.

Systematics
Family Buthidae C. L. Koch, 1837
Orthochiroides Kovařík, 1998 **stat**. **rev**.
(Figures 1–121, 130–133, 140–146, 166–167, 205–211; Tables 1–5)

Orthochiroides Kovařík, 1998: 115–120, figs. 1–5, 16–20, tab. 1–2; Fet & Lowe, 2000: 192; Kovařík, 2004: 23, 25, tab. 2; Fet & Soleglad, 2005: 11, tab. 2; Fet et al., 2005: 3, 13, tab. 1; Prendini & Wheeler, 2005: 481; Dupré, 2007:

8; Kovařík, 2009: 23; Kovařík et al., 2016a: 9; Lowe & Kovařík, 2021: 3.
Orthochirus (in part): Lourenço & Ythier, 2021: 337–339.

Type species. *Orthochiroides vachoni* Kovařík, 1998.

Diagnosis (adults). Total length of adults up to 24 mm (♂), or 34 mm (♀). Carapace strongly trapezoidal, posterior width/ anterior width > 2.2 (♂), > 2.3 (♀); surface densely, finely granulate, carinae indistinct; median eyes and ocular tubercle located in posterior 2/3 of carapace; preocular area in lateral view inclined downward from median eyes to anterior margin of carapace; 5 pairs of lateral eyes present, of which 2 pairs are either smaller or indistinct (Type 5 pattern; Loria & Prendini, 2014). Pectines hirsute, with fulcra, without enlarged basal teeth or enlarged basal middle lamellae. Pectinal tooth count range: 16–20 (♂), 14–18 (♀). Tergites I–VI either weakly mono- or tricarinate, or with carinae indistinct. Sternites IV–V, and maybe III, with prominent posterior median smooth patches; sternite VI antero-medial surface matte; posterior margins of sternites III–VI with fringes of regular, non-contiguous, enlarged, blunt denticles; spiracles hemi-elliptic or broadly slit-like. Metasomal segments relatively short, stout, either almost uniform in width or slightly incrassate posteriorly (metasoma V W/ metasoma I W < 1.1); carination moderately or weakly developed on metasoma I–II, weak or mostly masked by heavy cuticular morphosculpture on metasoma III–V; ventromedian surface of metasoma I granulate; lateral and ventral surfaces of metasoma IV–V either smooth and punctate, or rugose-reticulate. Antero-lateral corners of metasomal segments II–IV flush, not extended anteriorly and outwardly in wedge-shaped processes; metasomal segments II–III widening gradually in front of posterior margins. Posterior margins of tergite VII and metasomal segments I–III bearing fine fringes of microsetae. Telson with vesicle bulbous, aculeus shorter than vesicle, stout, strongly curved with tip angled > 90° relative to rostrocaudal axis; telson L/ D < 2.4, telson W/ metasoma V W > 0.5; subaculear tubercle absent. Chelicerae with typical buthid dentition (Vachon, 1963), fixed finger with two denticles on ventral surface. Pedipalps relatively short, chelae narrower than patella; patella with strongly costate dorsomedian and dorsoexternal carinae; chela manus with carinae V1, VA, D3 and D4 strongly costate, VA complete. Trichobothrial pattern neobothriotaxic type C (Vachon, 1974): femur with petite 'trichobothrium' d_2 absent on dorsal surface, d_1-d_3-d_4 in β-configuration (Vachon, 1975), e_1 proximal to d_5, positioned at base of femur; patella with petite 'trichobothrium' d_2 reduced or absent, d_3 located between dorsomedian and dorsointernal carinae, esb_2 near esb_1 (< 0.18 distance to em), em about midway between esb_2 and et; chela manus with Eb_2 proximal to Eb_1, V_1-V_2 axis slightly inclined internally, eb positioned on distal manus, not fixed finger; fixed finger with db positioned in middle 30-60% of finger, proximal to est; dentate margins of pedipalp fingers straight, without scalloping or lobe/ notch combination; movable finger equipped with 7–9 rows of median denticles
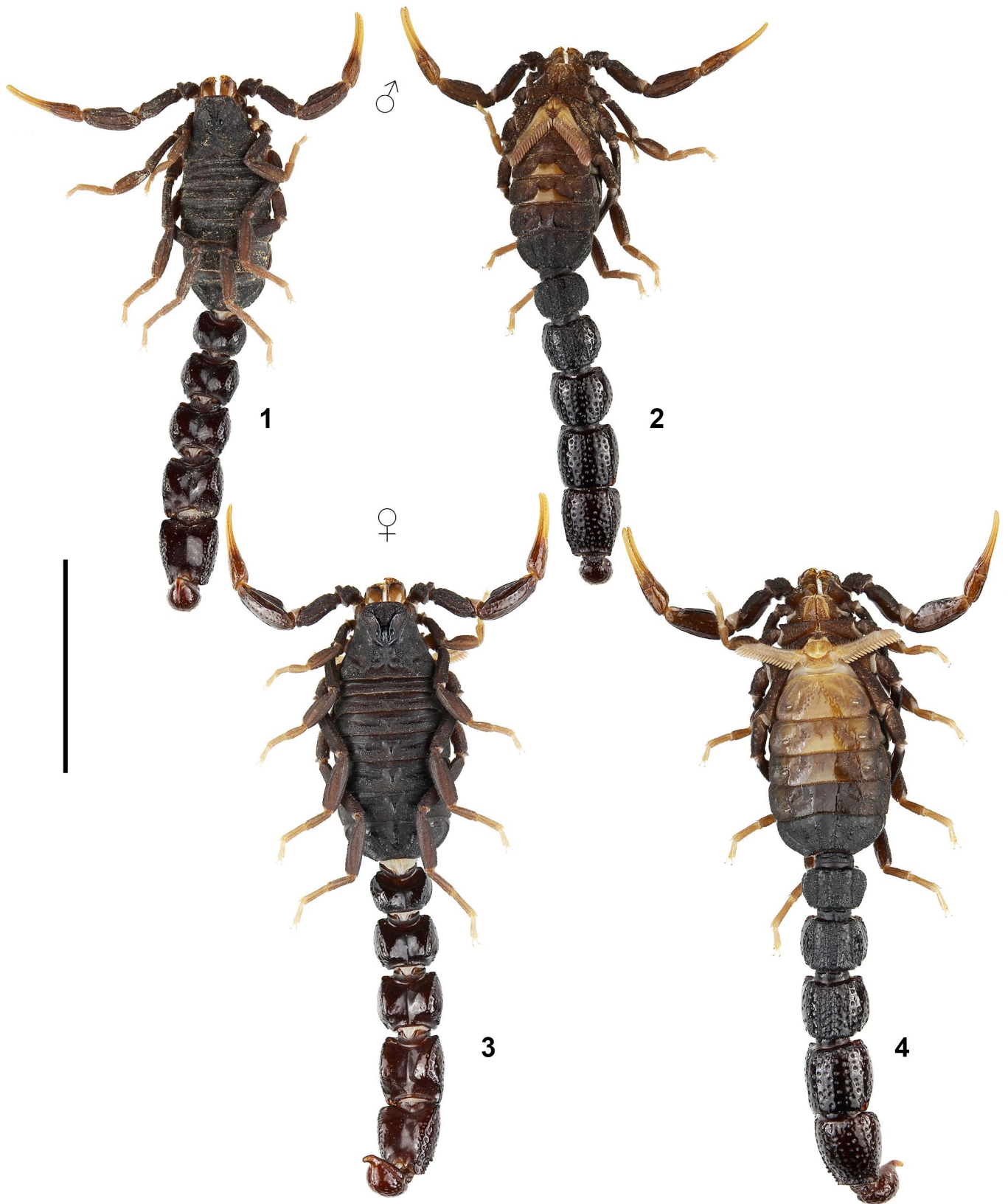
Figures 1–4: *Orthochiroides insularis*, Socotra Island. **Figures 1–2**. Male, dorsal (1) and ventral (2) views. **Figures 3–4**. Female, dorsal (3) and ventral (4) views. Scale bar: 10 mm.

arranged almost linearly, non-imbricated, each flanked by a single external (ED) and internal (ID) accessory denticle; 5 subterminal denticles present. Mid-ventral aspect of tarsomere II of legs sparsely setose with 1 or 2 rows of short spiniform setae; tibial spurs present on legs III–IV.

COMMENTS. Hemispermatophore characters are omitted from the generic diagnosis. We examined hemispermatophores from only one species, *O. somalilandus* **sp. n.** However, general features such as a sperm hemiduct divided into 3 lobes, and a folded flagellum with a broad, laminate pars recta and a narrow cylindrical pars reflecta, are probably present in other members of the genus. These features are highly conserved in all hemispermatophores that have been studied in genera of the '*Buthus*' group which includes *Orthochiroides* (cf. Fet et al, 2005).

Orthochiroides insularis (Pocock, 1899)
(Figures 1–4, 82, 87–94, 111–112, 119, 130–133, 140–142, 166, 205–211; Tables 1, 3)

Butheolus insularis Pocock, 1899: 8–9; Pocock, 1903: 180–181; Kraepelin, 1903: 565; Francke, 1977: 112; Vachon, 1979: 237.
Orthochirus insularis: Birula, 1917: 215.
Orthochirus bicolor insularis: Levy & Amitai, 1980: 94; El-Hennawy, 1992: 129; Fet & Lowe, 2000: 194; Kovařík, 2000: 64–66.
Orthochiroides insularis: Kovařík, 2004: 23.

TYPE LOCALITY AND TYPE REPOSITORY. Socotra, Mt. Raggit; BMNH.

TYPE MATERIAL EXAMINED. Yemen, **Socotra** Island, Hadibu Plain (Mt. Raggit, 1000 feet), 1♀ (holotype), leg. Grant and Forbes, BMNH No. 1899.7.4.180.
OTHER MATERIAL EXAMINED (FKCP). Yemen, **Socotra** Island, Qalansiyah env., Ditwah (lagoon), 23 m a. s. l., 12°41'42"N 53°30'08"E, 9.XII.2003, 1♂ (Figs. 1–2, 82, 87–90, 111), leg. D. Král; Gubbah village env., 7 m a. s. l., 12°36'35"N 53°46'56"E, 23.XI.2003, 1♀ (Figs. 3–4, 91–94, 112) 1juv., leg. D. Král; Qaariah village env., 11 m a. s. l., 12°38'05"N 54°12'39"E, 28.XI.2003, 1♂, leg. J. Farkač.

DIAGNOSIS (ADULT ♂♀). Total length of adults 22–32 mm. Petite 'trichobothria' d_2 on dorsal surfaces of pedipalp femur and patella reduced or absent. Chela smooth, carinae E and D1 weak or obsolete on manus. Pectinal tooth count: 18–19 (♂), 16–18 (♀). Movable finger of pedipalp chela with 7 rows of median denticles, flanked by 7 ID and 7 OD. Metasoma IV–V laterally and ventrally punctate, without carinae except for smooth, rugose dorsosubmedian carinae, and ventrolateral carinae on metasoma V which are anteriorly smooth and posteriorly denticulate. Metasoma III either laterally and ventromedially punctate (♂), or laterally punctate and ventromedially granulate-reticulate (♀). Punctae small with diameters less than the mean distance between their centroids,

together occupying much less area than smooth surfaces between them. Dorsal surfaces of all metasomal segments smooth, without punctae or granules. Aculeus much shorter than vesicle, aculeus L/telson L ~0.20. Color uniformly brown to black. Femur, patella and chela manus of pedipalp brown to black; chela fingers, and tibia and tarsomeres of legs yellowish brown to green. Tergites roughly granulated. Sternites IV–V with lateral surfaces matte, almost smooth. Sternite VII matte, almost smooth, with four distinct granulated carinae. Pedipalp, metasoma and telson glabrous, only metasoma V may have dorsolateral rows of setae, which can also occur on dorsal surface of telson. Moderately developed tibial spurs present on legs III and IV. Tarsomere I of legs I–III with 4–6 long setae in both sexes.

DISTRIBUTION. Yemen, north part of Socotra Island (Fig. 119).

COMMENTS. Fet & Lowe (2000: 194) listed "?*Orthochirus socotrensis*" cited by Francke (1977) as a possible *lapsus* and synonym of *Orthochirus bicolor insularis*. However, Francke (1977: 112) cited the presence of three endemic species of scorpion on Socotra Island: *Hemiscorpion socotranus* Pocock, 1899, *Butheolus insularis* Pocock, 1899 and *Orthochirus socotrensis* (Pocock). He omitted *Buthus socotrensis* Pocock, 1889 (= *Buthotus socotrensis* = *Hottentotta socotrensis*), also known from Socotra Island. It is possible that Francke cited '*Orthochirus socotrensis*' in error, instead of *Buthotus socotrensis*, as Pocock did not describe *Orthochirus socotrensis* (see also Vachon, 1979: 237).

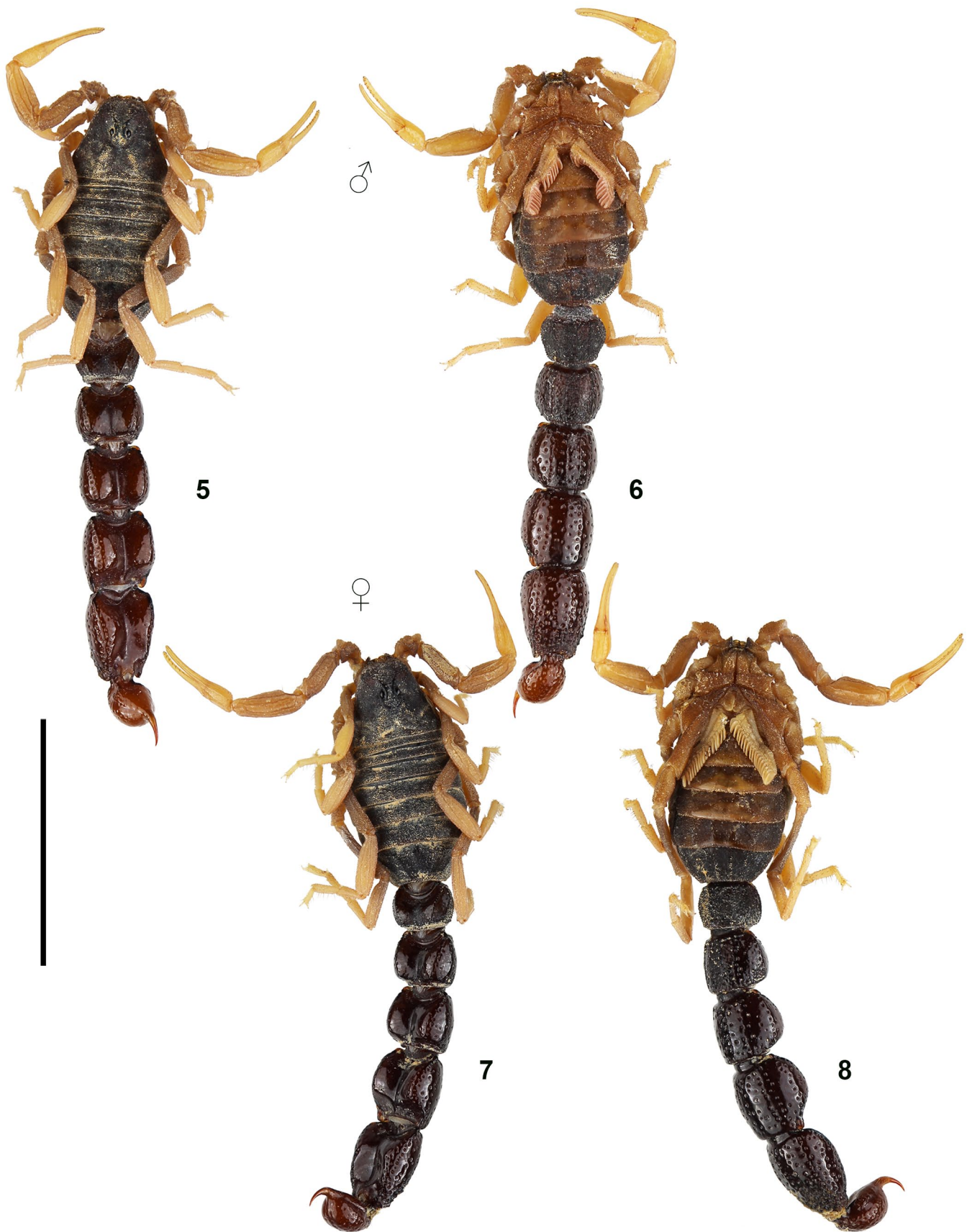### *Orthochiroides socotrensis* Kovařík, 2004
(Figures 5–8, 83, 95–102, 113–114, 119, 130–133, 140–141, 143, 205–211; Tables 1, 3)

Orthochiroides socotrensis Kovařík, 2004: 23–24; Fet & Kovařík, 2020: 3.

TYPE LOCALITY AND TYPE REPOSITORY. Yemen, Socotra Island, Noged plain, Qaareh (waterfall), 57 m a. s. l., 12°20'10"N 53°37'56"E; FKCP.

TYPE MATERIAL (FKCP). Yemen, **Socotra** Island, Noged plain, Qaareh (waterfall), 57 m a. s. l., 12°20'10"N 53°37'56"E, 5–6. XII.2003, 1♂ (holotype), leg. D. Král; Noged plain, Wadi Ireeh, 95 m a. s. l., 12°23'11"N 53°59'47", 6–7.XII.2003, 1♂ (paratype), leg. D. Král; Noged plain, 12.318°N 53.678°E, 250 m a. s. l., 1♂1♀2juvs. (paratypes), XI.1999, 1♀ (allotypic paratype), III.2001, leg. V. Bejček & K. Šťastný.

DIAGNOSIS (ADULT ♂♀). Total length of adults 24–32 mm. Petite 'trichobothria' d_2 on dorsal surfaces of pedipalp femur and patella reduced or absent. Chela smooth, carinae E and D1 weak or obsolete on manus. Pectinal tooth count 18–20 (♂), 16–18 (♀). Movable finger of pedipalp chela with 7 rows of median denticles, flanked by 7 ID and 7 OD. Metasoma III–V laterally and ventromedially punctate, without carinae except

Figures 5–8: *Orthochiroides socotrensis*. **Figures 5–6**. Male holotype, dorsal (5) and ventral (6) views. **Figures 7–8**. Female paratype, dorsal (7) and ventral (8) views. Scale bar: 10 mm.

Dimensions (mm)		*O*. *somalilandus* sp. n. ♂ holotype	*O*. *somalilandus* sp. n. ♀ paratype	*O. vachoni* ♂ Socotra
Carapace	L / W	3.29 / 3.90	3.86 / 4.97	3.03 / 3.74
Mesosoma	L	7.15	9.50	6.64
Tergite VII	L / W	1.87 / 3.93	2.29 / 4.82	1.87 / 3.76
Metasoma + telson	L	16.03	17.89	15.55
Segment I	L / W / D	1.91 / 2.65 / 2.19	2.11 / 3.00 / 2.54	1.84 / 2.49 / 2.20
Segment II	L / W / D	2.24 / 2.68 / 2.19	2.51 / 2.99 / 2.38	2.16 / 2.60 / 2.16
Segment III	L / W / D	2.44 / 2.75 / 2.28	2.68 / 3.15 / 2.43	2.27 / 2.74 / 2.32
Segment IV	L / W / D	2.94 / 2.86 / 2.31	3.23 / 3.13 / 2.46	2.75 / 2.83 / 2.36
Segment V	L / W / D	3.43 / 2.71 / 2.18	3.83 / 3.13 / 2.40	3.44 / 2.78 / 2.18
Telson	L / W / D	3.07 / 1.46 / 1.36	3.53 / 1.77 / 1.61	3.09 / 1.44 / 1.33
Pedipalp	L	8.46	9.69	8.29
Femur	L / W	1.90 / 0.99	2.18 / 1.02	1.86 / 0.81
Patella	L / W	2.75 / 1.30	3.21 / 1.49	2.75 / 1.20
Chela	L	3.81	4.30	3.68
Manus	W / D	0.98 / 0.95	1.16 / 1.14	0.92 / 0.91
Movable finger	L	2.51	2.73	2.43
Total	**L**	**26.47**	**31.25**	**25.22**

Table 1. Comparative measurements of *Orthochiroides somalilandus* **sp**. **n**. and *O. vachoni* specimens. Abbreviations: length (L), width (W, in carapace it corresponds to posterior width), depth (D).

for smooth, rugose dorsosubmedian carinae, and ventrolateral carinae on metasoma V which are anteriorly obsolete and posteriorly weakly denticulate. Punctae small with diameters less than the mean distance between their centroids, together occupying much less area than smooth surfaces between them. Dorsal surfaces of all metasomal segments smooth without punctae or granules. Aculeus much shorter than vesicle, aculeus L/telson L ~0.20. Color of mesosoma dark green, metasoma and telson reddish brown; pedipalps and legs yellow to yellowish green, lighter on more distal segments. Tergites roughly granulated. Sternites IV–V with lateral surfaces coarsely granulated. Sternite VII with moderately dense, coarse granulation throughout, and four granulated carinae. Pedipalp, metasoma and telson glabrous, only metasoma V may have dorsolateral rows of setae, which can also occur on dorsal surface of telson. Moderately developed tibial spurs present on legs III and IV. Tarsomere I of legs I–III with 4–6 long setae in both sexes.

DISTRIBUTION. Yemen, south part of Socotra Island (Fig. 119).

Orthochiroides somalilandus Kovařík & Lowe, **sp**. **n**.
(Figures 9–53, 118–121, 130–133, 140–141, 146, 167, 193–196, 205–211; Tables 1, 3)
http://zoobank.org/urn:lsid:zoobank.org:act:18E652AE-A564-4A2E-99D9-DBB31C5A85D1

TYPE LOCALITY AND TYPE REPOSITORY. Somaliland, Mader Mage village, between Eregavo and Maid, 10°48'03"N 47°17'46"E, 1389 m a. s. l. (Fig. 76); FKCP.

TYPE MATERIAL EXAMINED (FKCP). **Somaliland**, Mader Mage village, between Eregavo and Maid, 10°48'03"N 47°17'46"E, 1389 m a. s. l. (locality No. **18SD**), 23.VIII.2018, 3♂ (holotype and paratypes, DNA Nos. 1543, 1544) 1♀ (paratype), leg. F. Kovařík; 5 km S of Maid, 10°59'46"N 47°08'14"E, 182 m a. s. l. (Locality No. **18SF**; Fig. 77), 25.VIII.2018, 3♂ (paratypes, DNA No. 1539, Figs. 70–73), leg. F. Kovařík.

ETYMOLOGY. Named for its geographic distribution.

DIAGNOSIS (ADULT ♂♀). Total length of adults 24–32 mm. Petite 'trichobothria' d_2 on dorsal surfaces of pedipalp femur and patella reduced or absent. Chela with carinae E and D1 strongly costate, intercarinal surfaces sparsely granulate. Pectinal tooth count: 16–18 (♂), 15 (♀). Movable finger of pedipalp chela with 9 rows of median denticles, 9 ID and 9 OD. Metasoma V laterally and ventromedially rugose-reticulate and finely granulate. Metasoma III–IV laterally rugose-reticulate and finely granulate, ventromedially granulate. Inter-reticular depressions large, irregularly shaped, with diameters comparable to the mean distance between their centroids, together occupying much more area than the smooth or granular reticulations between them. Weak, finely granulated median lateral carinae present and complete on metasoma I–II, indistinct and masked by reticulate morphosculpture on metasoma III–IV. Dorsal surfaces of all metasomal segments smooth medially, granulate-reticulate or rugose-reticulate laterally; border between dorsal and dorsolateral surfaces of metasoma IV–V indistinct, not clearly demarcated by dorsosubmedian carina or abrupt transition
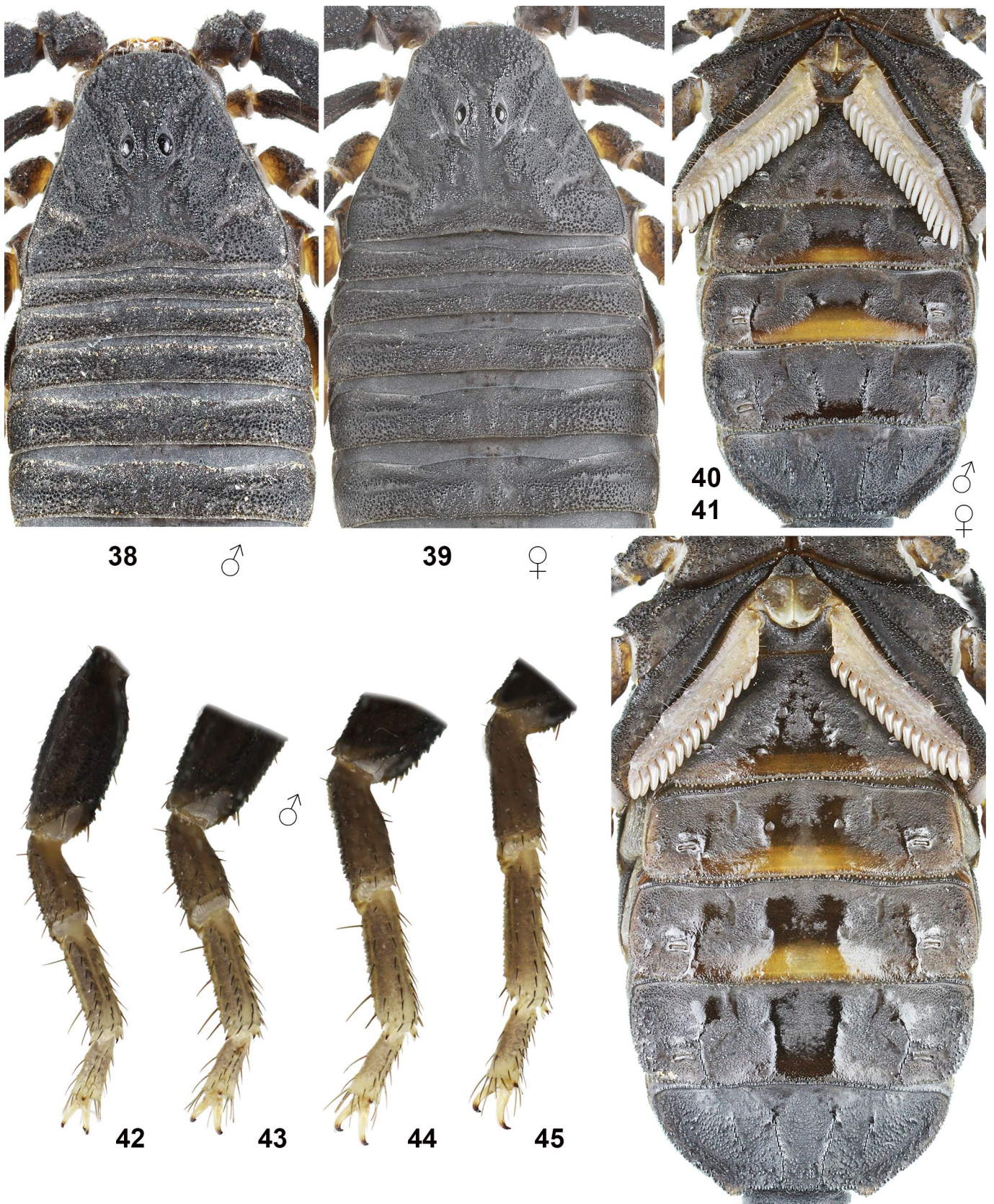
Figures 9–12: *Orthochiroides somalilandus* **sp**. **n**. **Figures 9–10**. Male holotype, dorsal (9) and ventral (10) views. **Figures 11–12**. Female paratopotype, dorsal (11) and ventral (12) views. Scale bar: 10 mm.
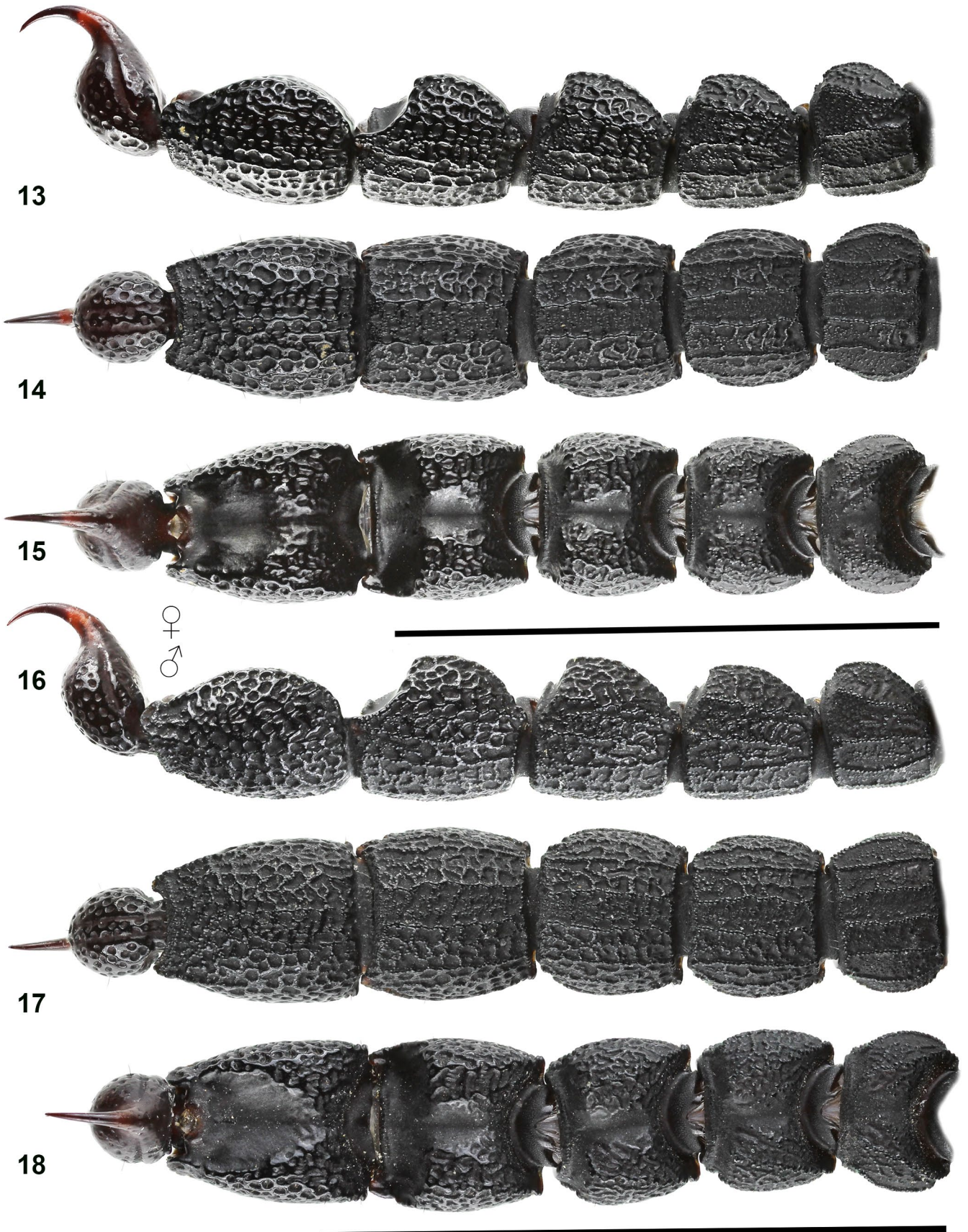
Figures 13–18: *Orthochiroides somalilandus* **sp. n**. **Figures 13–15**. Female paratopotype, metasoma and telson, lateral (13), ventral (14), and dorsal (15) views. **Figures 16–18**. Male holotype, metasoma and telson, lateral (16), ventral (17), and dorsal (18) views. Scale bars: 10 mm (13–15, 16–18).
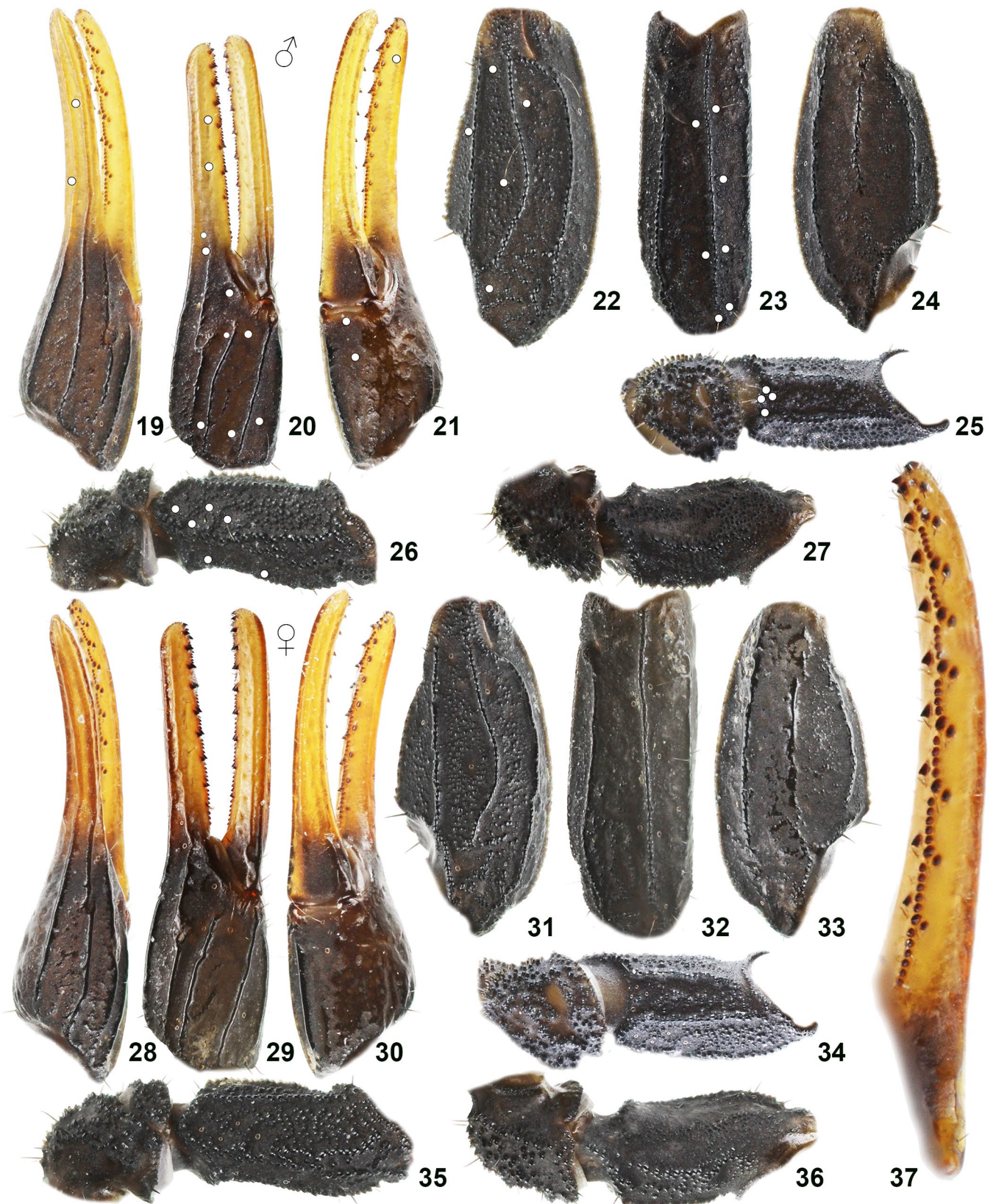
Figures 19–37: *Orthochiroides somalilandus* **sp. n.**, pedipalp. **Figures 19–27**. Male holotype, chela, dorsal (19), external (20), and ventral (21) views. Patella, dorsal (22), external (23) and ventral (24) views. Femur and trochanter, internal (25), dorsal (26), and ventral (27) views. **Figures 28–37**. Female paratopotype, chela, dorsal (28), external (29), and ventral (30) views. Patella, dorsal (31), external (32) and ventral (33) views. Femur and trochanter, internal (34), dorsal (35), and ventral (36) views. Movable finger dentation (37). Trichobothrial pattern indicated in Figures 19–23, 25–26 by white circles.

Figures 38–45: *Orthochiroides somalilandus* **sp**. **n**. **Figures 38**, **40**, **42–45**. Male holotype, carapace and tergites I–V (38), sternopectinal region and sternites (40), and left legs I–IV, retrolateral aspect (42–45). **Figures 39**, **41**. Female paratopotype, carapace and tergites I–V (39), sternopectinal region and sternites (41).

Figures 46–49: *Orthochiroides somalilandus* **sp**. **n**., male paratype, right hemispermatophore. **Figures 46**. Whole hemispermatophore. **Figures 47–49**. Capsule in posterior (47), convex compressed (48) and anterior (49) views. Scale bars: 1 mm (46), 200 μm (47–49).

in morphosculpture. Aculeus slightly shorter than vesicle, aculeus L/telson L > 0.30. Color uniformly black except for pedipalp chela fingers and tarsomeres of legs, which are yellow to yellowish brown. Tergites roughly granulated. Sternite VII densely granulated, with four granulated carinae. Pedipalp, metasoma and telson glabrous. Moderate to small tibial spurs present on legs III and IV. Tarsomere I of legs I–III with 3–4 long setae in both sexes.

DESCRIPTION. Total length of adults 24–32 mm in both sexes. For habitus, see Figs. 9–12, 50–51.
Coloration (Figs. 9–12, 50–51). Color uniformly black, except for pedipalp chela fingers and tarsomeres of legs which are yellow to yellowish brown. Telson reddish brown.
Carapace and mesosoma (Figs. 38–41). Carapace surface roughly granulated except for several smooth furrows. Superciliary carinae granulated, extending partially into preocular triangle. Tergites I–VI roughly granulated, with weak median and lateral carinae. Sternite VII densely granulated with four granulated carinae; other sternites finely granulated or shagreened in lateral areas. Sternite VI with median carinae granulated (♂), or smooth (♀), lateral carinae granulated in

both sexes. Glossy smooth patch present on median-posterior zone of sternites IV–VI (♂), or sternites III–VI (♀). Posterior margins of sternites III–VI (♂), or III–V (♀) equipped with rows of non-contiguous clavate or digitate denticles. Pectinal tooth count: 16–18 (3 x 16, 3 x 17, 4 x 18) (♂), 15 (♀). Female pectine teeth notably shorter than male teeth, mid-pectine sensillar margin L/ tooth W 1.63 (♀), 2.45 (♂).
Hemispermatophore (Figs. 46–49). Flagelliform. Trunk narrow, elongate, broadened proximally. Flagellum folded, with thicker, laminate pars recta, 0.45 times length of trunk, and thinner, cylindrical, hyaline pars reflecta, 0.61 times length of trunk. Capsule short, 0.15 times length of trunk. Sperm hemiduct divided into 3 lobes; posterior lobe longest, lanceolate; median lobe shortest, laminate; median and anterior lobes apically acuminate. Basal lobe an apically curved hook with a broad base.
Metasoma and telson (Figs. 13–18). Metasoma I–II with 10 granulated carinae. Metasoma III–IV without distinct median lateral carinae. Metasoma V with dorsosubmedian carinae smooth, rugose, irregular; ventrolateral carinae weak, granulated, restricted to posterior third of segment, other carinae absent. Metasoma I with intercarinal surfaces finely

Figures 50–51. *Orthochiroides somalilandus* **sp**. **n**., paratypes male (50) and female (51) in vivo (laboratory photographs on standard background).

Figures 52–53: *Orthochiroides somalilandus* **sp. n.**, localities. **Figure 52**. Type locality, Somaliland, Mader Mage vill., between Eregavo and Maid. **Figure 53**. Somaliland, 5 km S of Maid.

granulate. Metasoma III–IV laterally rugose-reticulate and finely granulate, ventromedially finely granulate. Metasoma V laterally and ventromedially rugose-reticulate, finely granulate in posterior ventral area. Reticulations on metasoma III–V thinner and partially granulated in male, thicker and polished in female. Dorsal surfaces of metasoma I–IV smooth medially, of metasoma V smooth posterio-medially; lateral areas of dorsal surfaces granulate on segment I, granulate reticulate on II, rugose-reticulate on III–V. Entire metasoma and telson glabrous. Telson smooth and punctate.

Pedipalps (Figs. 19–37). Petite 'trichobothrium' d_2 on dorsal surface of pedipalp femur absent. Femur with five granulated carinae, intercarinal surfaces densely granulated. Patella with seven moderately to strongly costate, smooth or granulated carinae; intercarinal surfaces with sparse fine granulation, or almost smooth. Chela with six complete, strongly costate, smooth or weakly crenulate carinae (V1, VA, E, D1, D3 and D4), with D1, D3 and D4 extending along full length of fixed finger; intercarinal surfaces with sparse fine granulation, or almost smooth. All pedipalp segments glabrous, bearing only several setae. Movable fingers with 9 rows of denticles, 9 ID and 9 OD.

Legs (Figs. 42–45). Legs III–IV with moderate to small tibial spurs. Femur with four granulated carinae; patella with five carinae. Patella with only a few macrosetae. Tibia with macrosetae on the retrosuperior aspect of legs I–II. Tarsomere I of legs I–III with 3–4 long macrosetae in both sexes, of legs IV with 2 setae. Tarsomeres I–II of all legs with two irregular rows of macrosetae on proinferior and retroinferior aspects.

Measurements. See Table 1.

COMMENTS ON LOCALITY AND LIFE STRATEGY. The type locality **18SD** is a montane slope with trees and bushes (Fig. 52, fig. 82 in Kovařík et al., 2019a: 15 and fig. 139 in Kovařík & Lowe, 2021: 25) and is also the type locality of the scorpionid *Pandinurus fulvipes* Kovařík et al., 2019, and buthid *Hottentotta nigrimontanus* Kovařík & Lowe, 2021. All specimens were collected among rocks near Mader Mage village at an approximate elevation of 1,389 m a. s. l. At this locality, the first author recorded a minimum nighttime temperature of 24 ºC. The minimum recorded humidity was 37%. The locality **18SF** is in foothills at the border between sandy semi-desert and rocky terrain (Fig. 53 and fig. 89 in Kovařík & Lowe, 2020: 16). Type specimens were collected at night by UV detection on rocks, together with *Compsobuthus maidensis* Kovařík, 2018 and *Leiurus gubanensis* Kovařík & Lowe, 2020.

Orthochiroides vachoni Kovařík, 1998
(Figures 54–81, 84–86, 103–110, 115–117, 119, 130–133, 140–141, 144–145, 205–211; Tables 1, 3)

Orthochiroides vachoni Kovařík, 1998: 117–120, figs. 1–5, 16–20, tab. 1–2; Fet & Lowe, 2000: 193; Kovařík, 2002: 9; Kovařík, 2003: 135, 142, tab. 1; Kovařík, 2004: 24.
Orthochirus vachoni: Lourenço & Ythier, 2021: 344, figs. 16–20.

TYPE LOCALITY AND TYPE REPOSITORY. Somalia, Sar Uanle, about 20 km south from Chisimaio, 00°29'48"S 42°25'30"E; MZUF.

TYPE MATERIAL EXAMINED. **Somalia**, Sar Uanle, about 20 km South from Chisimaio, 00°29'48"S 42°25'30"E, (for locality details see Messana et al., 1977, and Vanini et al., 1977), 18♂ (holotype and paratypes Nos. 1–17), 11♀ (paratypes Nos. 18–27), 9 juvs. (paratypes Nos. 28–36). Holotype (No. 533), allotypic paratype (No. 537), and paratypes Nos. 1–9, 20–29, 31–35 (No. 539) are in MZUF. Other paratypes are in BMNH, FKCP, MNHN, NMPC, SMFD, ZMHB, ZMUH (see Kovařík, 1998).

OTHER MATERIAL EXAMINED. **Yemen**. Socotra Island, XI.2000, 1♂, leg. V. Bejček & K. Šťastný, FKCP.

DIAGNOSIS (ADULT ♂♀). Total length of adults 24–35 mm. Petite 'trichobothrium' d_2 on dorsal surface of pedipalp femur absent; petite 'trichobothrium' d_2 on dorsal surface of pedipalp patella reduced or absent. Chela with carinae E and D1 strongly costate, intercarinal surfaces sparsely granulate or tuberculate. Pectinal tooth count: 17–20 (♂), 14–18 (♀). Movable finger of pedipalp chela with 8–9 rows of median denticles, 9 ID and 9 OD. Metasoma III–V laterally and ventromedially rugose-reticulate and finely granulate. Inter-reticular depressions large, irregularly shaped, with diameters comparable to the mean distance between their centroids, together occupying much more area than the smooth or granular reticulations between them. Lateral median carinae present in male, weak, finely granulated, complete on metasoma I–II, restricted to posterior half of segment on metasoma III–IV. Dorsal surfaces of all metasomal segments weakly rugose. Metasoma IV–V with border between dorsal and dorsolateral surfaces clearly demarcated by dorsosubmedian carina, and in male by abrupt transition in morphosculpture. Aculeus moderately shorter than vesicle, aculeus L/telson L ~0.25. Color uniformly brown to black; femur, patella and chela manus of pedipalps brown; chela fingers, and tibia and tarsomeres of legs yellow to yellowish brown. Tergites roughly granulated. Sternite VII densely granulated, with four granulated carinae. Pedipalp, metasoma and telson glabrous. Moderate to small tibial spurs present on legs III and IV. Tarsomere I of legs I–III with 3–6 long setae in both sexes.

DISTRIBUTION. Somalia, Yemen (Socotra Island) (Fig. 119).

COMMENTS. The two widely disjunct records of *O. vachoni*: (i) an extensive type series including specimens of both sexes, and juveniles, from the type locality in southern Somalia (Kovařík, 1998), and (ii) a single male specimen from Socotra Island (Kovařík, 2004), are puzzling from a biogeographic perspective. Socotra Island is separated from the type locality by a distance of ca. 1,900 km, and isolated from the nearest mainland point on the coast of Africa by a 240 km wide marine barrier (Fig. 119). Its fauna exhibits high endemism (Cheung et al., 2006; Purchart et al., 2020). The other two species of *Orthochiroides* found on
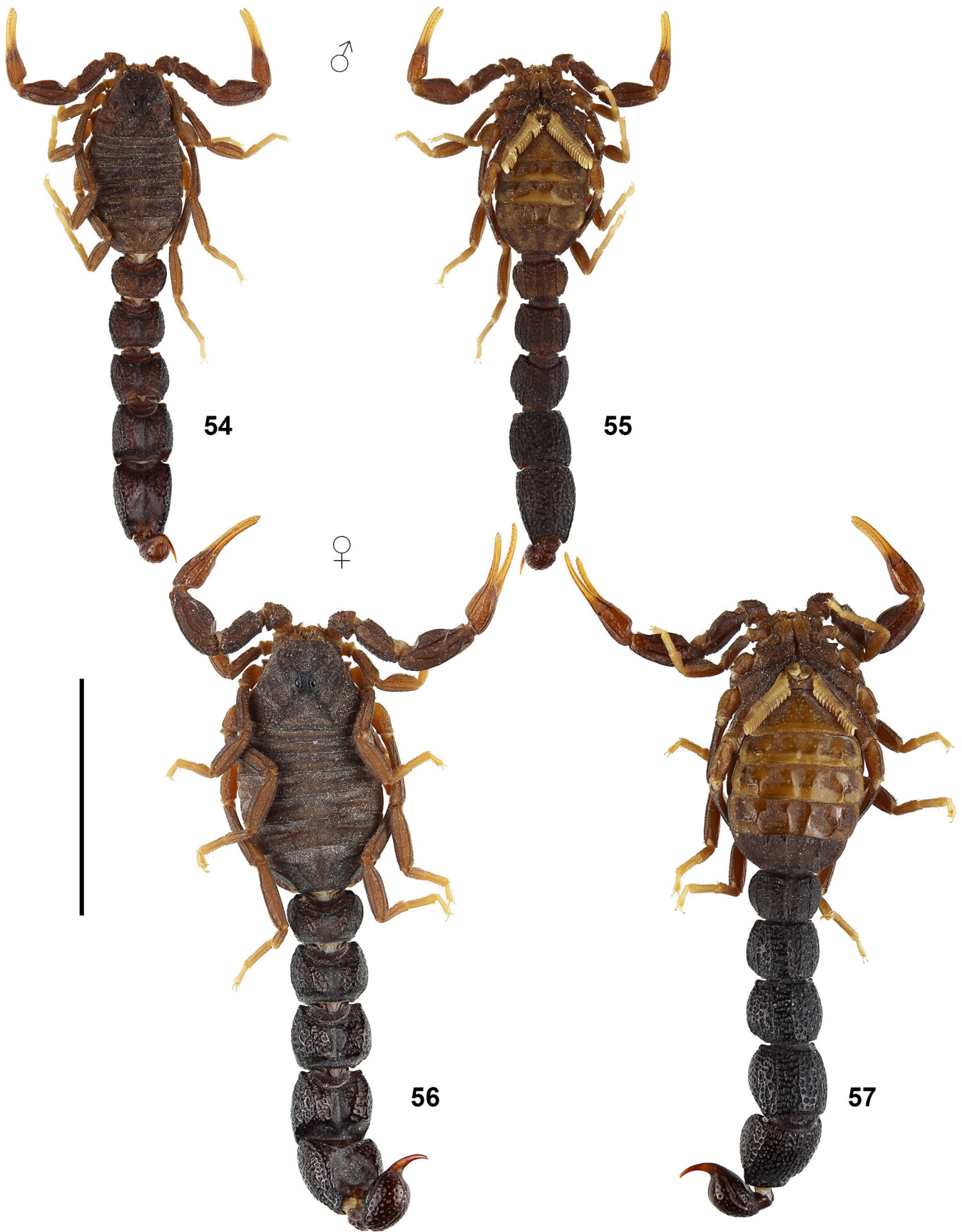
Figures 54–57: *Orthochiroides vachoni*, paratypes, FKCP. **Figures 54–55**. Male, dorsal (78) and ventral (79) views. **Figures 56–57**. Female, dorsal (80) and ventral (81) views. Scale bar: 10 mm.

Figures 58–59. *Orthochiroides vachoni*, male from Socotra, dorsal (58) and ventral (59) views.

Socotra (*O. insularis* and *O. socotrensis*) are endemic, as are two other Socotra scorpions, *Hemiscorpius socotranus* Pocock, 1889 and *Hottentotta socotrensis* (Pocock, 1889). This suggests that '*O. vachoni*' from Socotra might also be an endemic species different from *O. vachoni* on the mainland. However, the Socotra specimen is virtually identical to all paratype males of *O. vachoni* that we have examined (Figs. 58–81, Tab. 1). There are only a few minor differences that lie well within the scope of intraspecific variation typical for other buthids (i.e., sternite VII fine granulation slightly more intense; metasoma III-IV median lateral carinae slightly less visible and partially obscured in both by strong reticulate morphosculpture; small morphometric differences in metasoma V). In our opinion, these

differences are insufficient for the diagnosis of a new species. The other mainland African species *O. somalilandus* **sp**. **n**. differs more from *O. vachoni*, than does the specimen from Socotra. The collection of an extensive type series of *O. vachoni* from southern Somalia (Kovařík, 1998), and the presence of a closely similar species in Somaliland, indicate that this species occurs naturally on the mainland. We cannot exclude the possibility that the Socotra record is spurious and possibly an introduction by human transport. Other non-endemic flora and fauna occur on or have been introduced to the island (e.g., Hůla & Niedobová, 2020; Senan et al., 2010; Witt et al., 2020). The range of distribution of *O. vachoni* in Somalia is unknown. It may not be confined to its type locality, and could extend further

Figures 60–63. *Orthochiroides vachoni*, male from Socotra, metasoma V and telson lateral (60), and metasoma and telson, lateral (61), dorsal (62), and ventral (63) views. Scale bar: 10 mm (61–63).

up the coast closer to Socotra. Without further information, we take a conservative approach and provisionally classify the Socotra record as *O. vachoni*.

In their paper synonymizing *Orthochiroides* with *Orthochirus*, Lourenço & Ythier (2021) examined a single male paratype of *Orthochiroides vachoni* deposited in MNHN, and illustrated its metasomal segment V and telson in lateral view (Lourenço & Ythier, 2021: 344, fig. 20). They depicted the morphosculpture on the lateral surface of metasoma V as consisting of numerous small, rounded depressions or punctae of uniform size and shape, with diameters much less than the mean distance between their centroids, that together occupy much less area than the smooth surfaces between them. This is similar to the punctate morphosculpture on metasoma V of most species of *Orthochirus*. Their illustration differs from the illustration of a rugose-reticulate morphosculpture on the lateral surface

of the male holotype published in the original description of *O. vachoni* (Kovařík, 1998: 117, fig. 1). In that figure, the depressions are depicted as more irregular in size and shape, including larger diameters comparable to the mean distance between their centroids, together occupying as much or more area than the surface between them. Kovařík (1998: 117–119, figs. 4–6) described the larger depressions on the metasoma of *O. vachoni* and emphasized their difference from the punctae of *Orthochirus*. This morphosculpture is documented again here photographically for comparison to fig. 20 of Lourenço & Ythier (2021) (cf. Figs. 60–63, 84–86). Kovařík (1998) analyzed the entire type series of *O. vachoni* consisting of 38 specimens, including the paratype deposited in MNHN, and did not report any examples of fine punctate morphosculpture on the metasoma. We regard fig. 20 of Lourenço & Ythier (2021) to be a gross misrepresentation of the true anatomy of *O. vachoni*.

Figures 64–81: *Orthochiroides vachoni*, male from Socotra. **Figures 64–75**. Pedipalp. Chela, dorsal (64), external (65), and ventral (66) views. Patella, dorsal (67), external (68) and ventral (69) views. Femur and trochanter, internal (70), dorsal (71), ventral (72), and external (73) views. Movable (74) and fixed (75) finger dentation. Trichobothrial pattern indicated in Figures 64–68, 70–71 by white circles. **Figures 76–77**. Carapace and tergites I–VI (76), sternopectinal region and sternites (77). **Figures 78–81**. Right legs I–IV, retrolateral aspect.
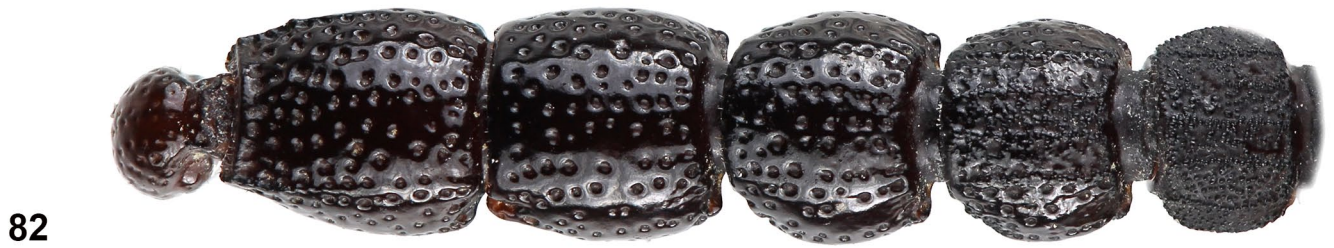
82

Orthochiroides insularis

83

Orthochiroides socotrensis

♂
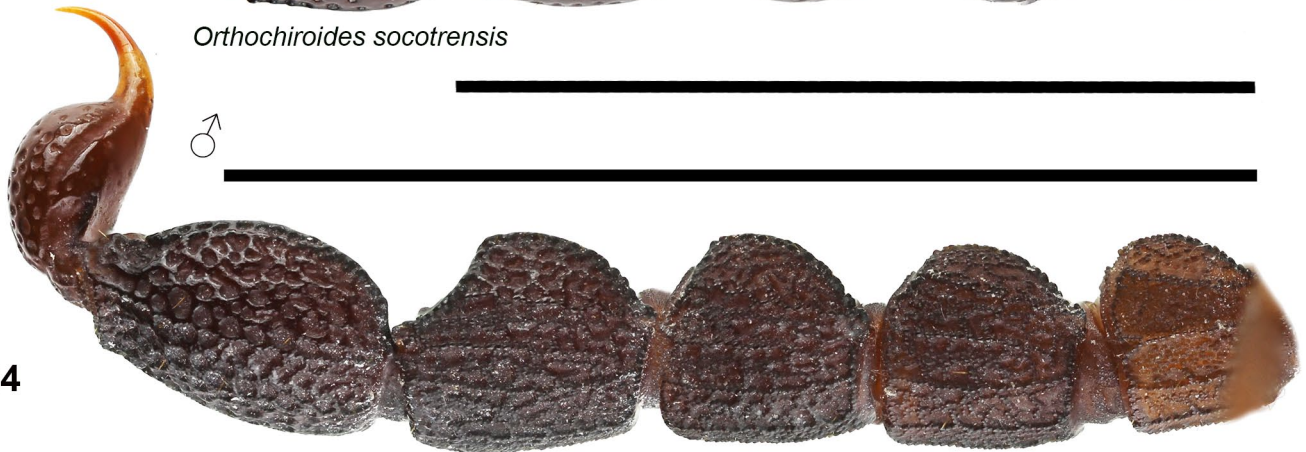
84

85

86

Orthochiroides vachoni

Figures 82–86: *Orthochiroides*, males. **Figures 82**. *O. insularis*, metasoma and telson, ventral view. **Figures 82**. *O. socotrensis*, holotype, metasoma and telson ventral view. **Figures 84–86**. *O. vachoni*, paratype, metasoma and telson, lateral (84), ventral (85), and dorsal (86) views. Scale bars: 10 mm (82–83, 84–86).

Orthochiroides insularis (Pocock, 1899)   *O. socotrensis* Kovařík, 2004   *O. vachoni* Kovařík, 1998

O. insularis   *O. socotrensis*   *O. vachoni*   *O. somalilandus* **sp. n.**

Figures 87–118: Comparation of *Orthochiroides* spp., pedipalp chela dorsal and external (87–88, 91–92, 9–96, 99–100, 103–104, 107–108), patella dorsal and external (89–90, 93–94, 97–98, 101–102, 105–106, 109–110), and movable finger dentation (111–118). **Figures 87–94, 111–112**. *Orthochiroides insularis*, Socotra Island, male (87–90, 111) and female (91–94, 112). **Figures 95–102, 113–114**. *O. socotrensis*, male holotype (95–98, 113) and female paratype (99–102, 114). **Figures 103–110, 115–117**. *O. vachoni*, male paratype No. 11 (103–106, 115), female paratype No. 18 (107–110, 116) and male from Socotra (117). **Figure 118**. *O. somalilandus* **sp. n.**, female pratype.
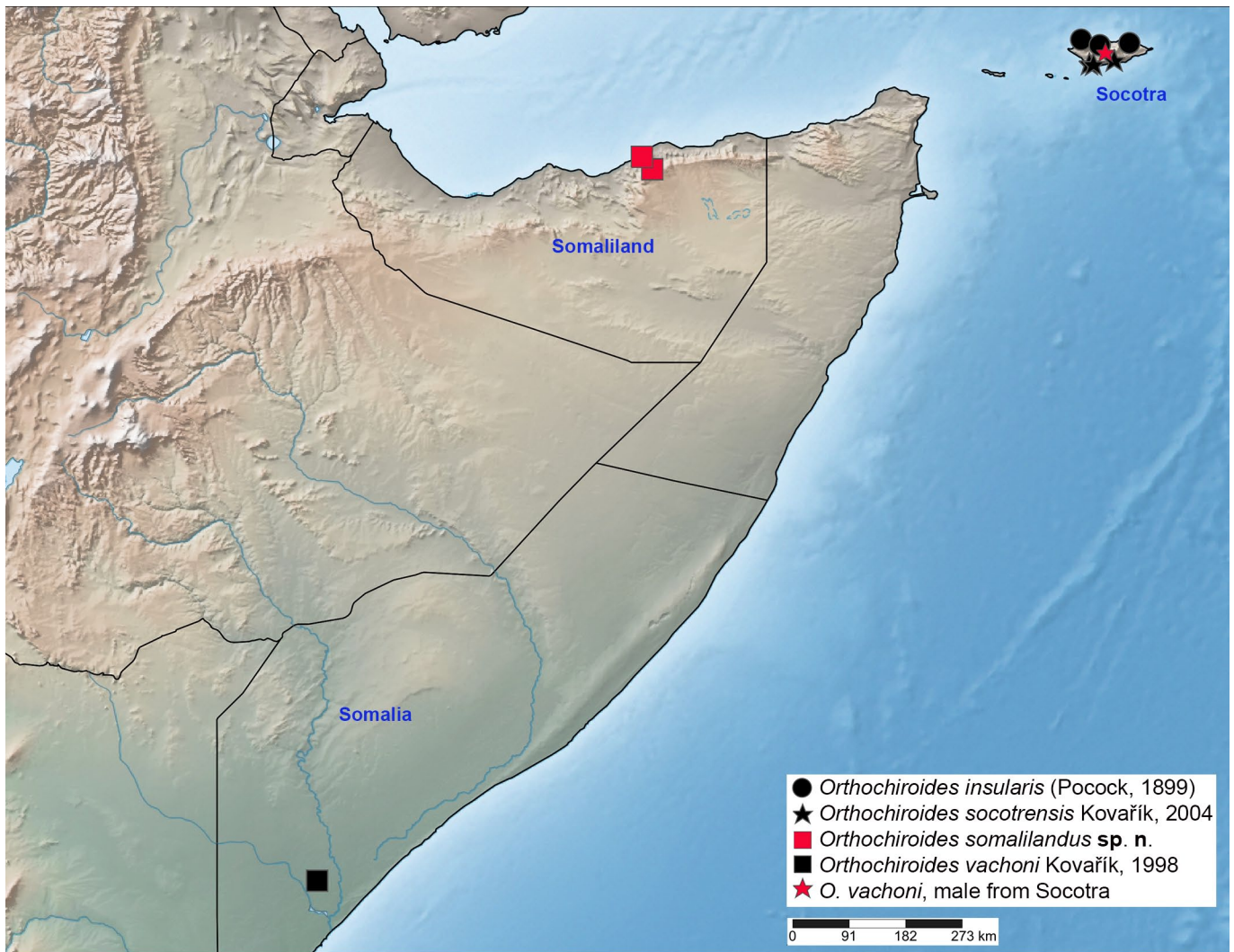
Figure 119. Geographic distribution of *Orthochiroides* spp.

Key to species of *Orthochiroides*

1. Movable finger of pedipalps with 7 rows of median denticles, 7 ID and 7 OD (Figs. 111–114); metasoma IV–V of adults ventrally smooth and punctate; punctae on ventral surface of metasoma V small, with diameters less than mean distance between their centroids, occupying less area than smooth surfaces between them (Figs. 82–83); pedipalps more slender, patella L/W 2.5–3.0 ……...........2
– Movable finger of pedipalps with 8–9 rows of median denticles, 9 ID and 9 OD (Figs. 115–118); metasoma IV–V of adults ventrally rugose-reticulate; inter-reticular depressions or lacunae on ventral surface of metasoma V large, irregularly shaped, with diameters comparable to mean distance between their centroids, occupying more area than raised reticular surfaces (Figs. 13–18, 60–63, 84–86); pedipalps more stout, patella L/W 2.1–2.3 3

2. Pedipalps with patella and chela manus brown or black, darker than fingers (Figs. 87–94); sternite VII matte, almost smooth .... *O. insularis* (Pocock, 1899)
– Pedipalps with patella and entire chela yellow (Figs. 95–102); sternite VII coarsely granulated .... *O. socotrensis* Kovařík, 2004

3. Border between dorsomedian and dorsolateral surfaces of metasoma IV–V distinct, demarcated by dorsosubmedian carina; dorsal surfaces of metasoma III–V weakly rugose laterally (Fig. 86); metasoma IV ventromedially rugose-granulate (Fig. 85). .... *O. vachoni* Kovařík, 1998
– Border between dorsomedian and dorsolateral surfaces of metasoma IV–V indistinct, not demarcated by dorsosubmedian carina; dorsal surfaces of metasoma III–V strongly rugose or rugose-reticulate laterally (Fig. 18); metasoma IV ventromedially granulate (Fig. 17). …………………………………… *O. somalilandus* **sp**. **n**.

Morphological characters separating *Orthochiroides* Kovařík, 1998 from *Orthochirus* Karsch, 1891

Kovařík (1998: 116) separated *Orthochiroides* (then monotypic, with type species *Orthochiroides vachoni*) from *Orthochirus* on the basis of telson shape (i.e., bulbous or "*inflated*" vs. slender respectively) and morphosculpture of metasoma V (larger "*punctae*" occupying a major part of the surface, vs. smaller punctae occupying a minor part of a smooth surface, respectively). The posterior metasoma of *Orthochiroides vachoni* exhibits a distinctive and unique rugose-reticulate morphosculpture. The "*punctae*" of Kovařík (1998) are herein described as inter-reticular depressions or lacunae. Kovařík (1998: 119–120) also reported an ontogenetic character, in which the metasomal segments of juvenile *Orthochiroides vachoni* are granulated, and lack the reticulate morphosculpture and depressions characteristic of adults. In contrast, the smooth, punctate morphosculpture of the metasomal segments typical of adult *Orthochirus* is already well expressed in juveniles of that genus. Other characters separating *Orthochiroides* from *Orthochirus* were implicit in the generic diagnosis of Kovařík (1998: 116): e.g., "*four pairs of lateral eyes*" and "*six pronounced keels on the tibia of pedipalps*" (= 6 strong costate carinae on the pedipalp chela).

Kovařík (2004: 23–24) extended the genus *Orthochiroides* to encompass *Butheolus insularis* Pocock, 1899, and described another species, *Orthochiroides socotrensis* Kovařík, 2004. The metasomal segments of these two species exhibit a smooth, punctate morphosculpture, similar to that of *Orthochirus*. In a revised diagnosis of *Orthochiroides*, Kovařík (2004: 23) characterized metasoma IV–V as "*ventrally punctate*" in a broad sense to also cover the different rugose-reticulate condition in *Orthochiroides vachoni*. The only character mentioned that separated *Orthochiroides* from *Orthochirus* was the shape of the telson.

Lourenço & Ythier (2021: 339) dismissed almost all of the diagnostic characters proposed for the genus *Orthochiroides* by Kovařík (1998, 2004) as being "*without any generic value*", discussing only two possibly valid characters: (1) four pairs of lateral eyes, which they rejected because they observed only three pairs in the male paratype that they examined; and (2) a bulbous telson, which they confirmed in their male paratype, but dismissed as "*not sufficient for the definition of a genus*". In the first case, surveys of the comparative anatomy of lateral eyes in buthids (Loria & Prendini, 2014; Yang et al., 2013) found that five pairs were present in the majority of genera and species, while a minority had reduced counts of of 2–4 pairs. Intraspecific variation in lateral eye counts could also occur. Earlier studies may have underestimated the counts, as the typical 5-eye pattern includes 3 larger ocelli (PLMa, MLMa, ALMa) which are readily visible, plus two smaller ocelli (PDMi, ADMi) which are more difficult to detect ('Type 5' configuration of Loria & Prendini, 2014). We re-examined the lateral eyes of *Orthochiroides* and detected up to five pairs in a Type 5 configuration, although in some cases only 3 or 4 were discernible (either PDMi or ADMi
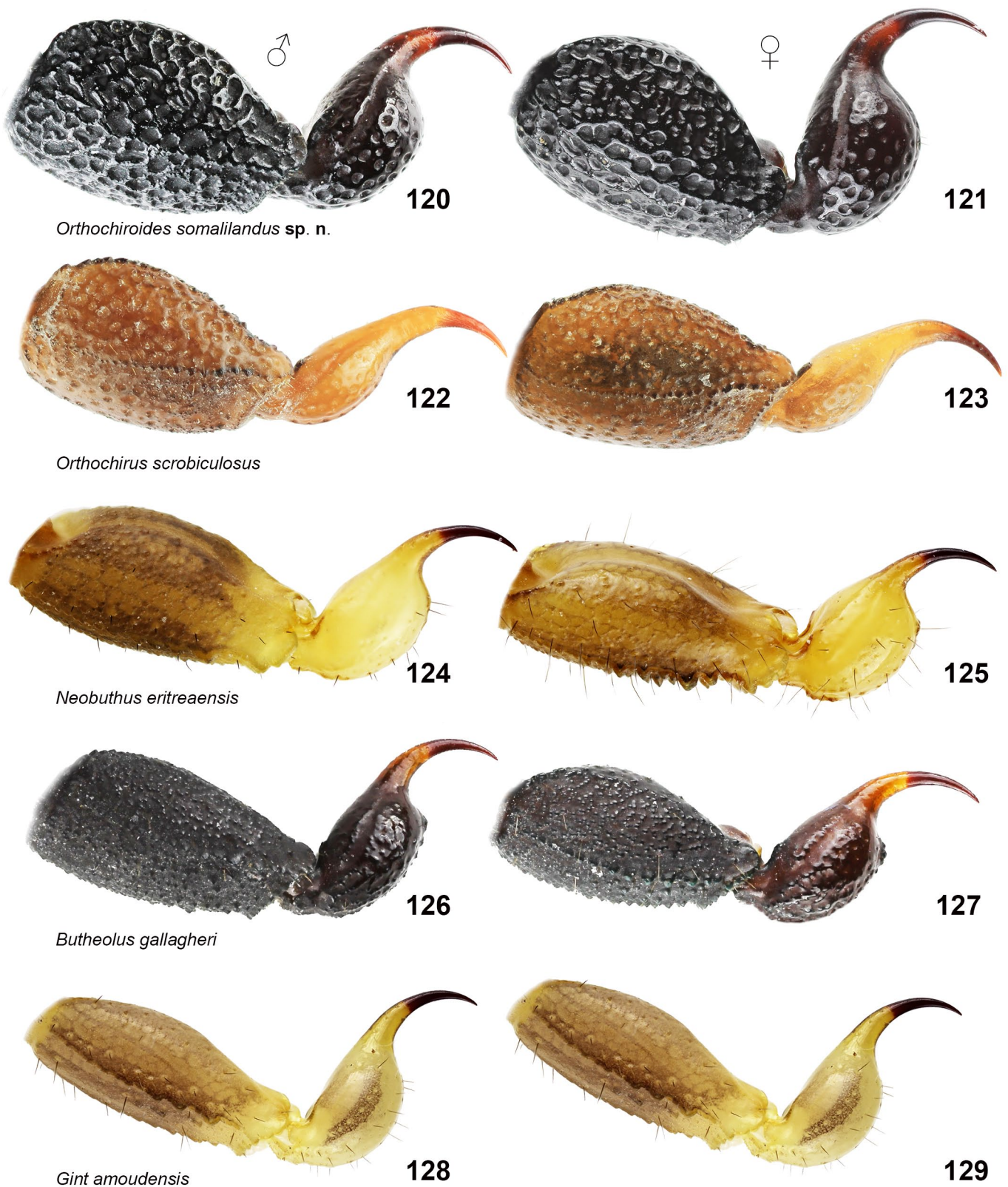
may be indistinct). We therefore consider Type 5 to be the basic pattern in *Orthochiroides*, a pattern that is also found in *Orthochirus*. We agree that this character does not separate *Orthochiroides* from *Orthochirus*. However, it does contribute some diagnostic value by excluding those buthid genera with 2–4 pairs of lateral eyes. In the second case, although the difference between telson shapes of *Orthochiroides* and *Orthochirus* was confirmed by Lourenço & Ythier (2021: 339), they nevertheless rejected it as a diagnostic character for *Orthochiroides*. Below, we examine this character and six other characters that we propose for the differential diagnosis of *Orthochiroides* vs. *Orthochirus*. Character numbers and states refer to the list in Table 5.

(i) Carapace shape: *Orthochiroides*: strongly trapezoidal, posterior width/ anterior width > 2.2 (♂), > 2.3 (♀); *Orthochirus*: moderately trapezoidal, posterior width/ anterior width < 2.2 (♂), < 2.3 (♀) (character 6, states 2 and 1).

The dorsal profile of a scorpion carapace varies from being almost parallel-sided, to having lateral margins anteriorly convergent. The former shape has been loosely termed 'sub-rectangular' and the latter 'trapezoidal', although the distinction is subjective without quantitative rules for determining which is applicable. In order to objectively compare carapace shapes of *Orthochiroides* and *Orthochirus*, we measured two morphometric ratios, carapace W/L and carapace posterior W/ anterior W. These ratios parametrize the possible ranges of trapezoidal geometries, mapping them into a 2D morphospace. More 'strongly' trapezoidal carapaces are characterized by higher values of these ratios. We analyzed and compared the ratios for *Orthochiroides* (4 spp., 100% of named species) and *Orthochirus* (45 spp., 85% of named species). In Figs. 130–131, ratios for different species of male and female *Orthochiroides* and *Orthochirus* are shown in bivariate scatter plots. Across *Orthochirus* species, posterior W/ anterior W was positively correlated with W/ L (P = 0.00014) in females, but not in males (P = 0.111). In both sexes of *Orthochiroides*, the ratio of posterior W/ anterior W tended to be higher for higher values of W/L, although the trend was not statistically significant given the small number of species. However, the important result for differential diagnosis is that the morphospace domains occupied by carapaces of *Orthochiroides* and *Orthochirus* are disjunct in both sexes. The two genera can be reliably separated by threshold values of the ratio of posterior W/ anterior W.

(ii) Telson shape: *Orthochiroides*: vesicle bulbous, telson L/D < 2.5 (♂♀), telson W/ metasoma V W < 0.5 (♀); *Orthochirus*: vesicle slender, pyriform, telson L/D > 2.5 (♂♀), telson W/ metasoma V W > 0.5 (♀) (character 40, states 1 and 2; character 43, states 0 and 1) (cf. Kovařík, 1998: 116: *Orthochiroides*, "*differs in shape of the telson, which is highly inflated*").

The morphometric ratio of telson L/ telson D is a measure of telson elongation. Bulbous telsons have lower values, and slender telsons higher values. We analyzed and compared the ratio for *Orthochiroides* (4 spp., 100% of named species) and

Orthochiroides somalilandus **sp**. **n**.

Orthochirus scrobiculosus

Neobuthus eritreaensis

Butheolus gallagheri

Gint amoudensis

Figures 120–129: Comparison of metasoma V and telson of five ingroup genera in lateral view. **Figures 120–121**. *Orthochiroides somalilandus* **sp**. **n**., male holotype (120) and female paratopotype (121). **Figures 122–123**. *Orthochirus scrobiculosus* (Grube, 1873), male topotype (NMB, 122) and female holotype (123). **Figures 124–125**. *Neobuthus eritreaensis* Lowe et Kovařík, 2016, male (124) and female (125) paratypes. **Figures 126–127**. *Butheolus gallagheri* Vachon, 1980, male (126) and female (127) from Oman, Mirbat, 17°02.19'N 54°38.75'E, 54 m a. s. l. (FKCP). **Figures 128–129**. *Gint amoudensis* Kovařík et al., 2018, male holotype (128) and female paratype (129).
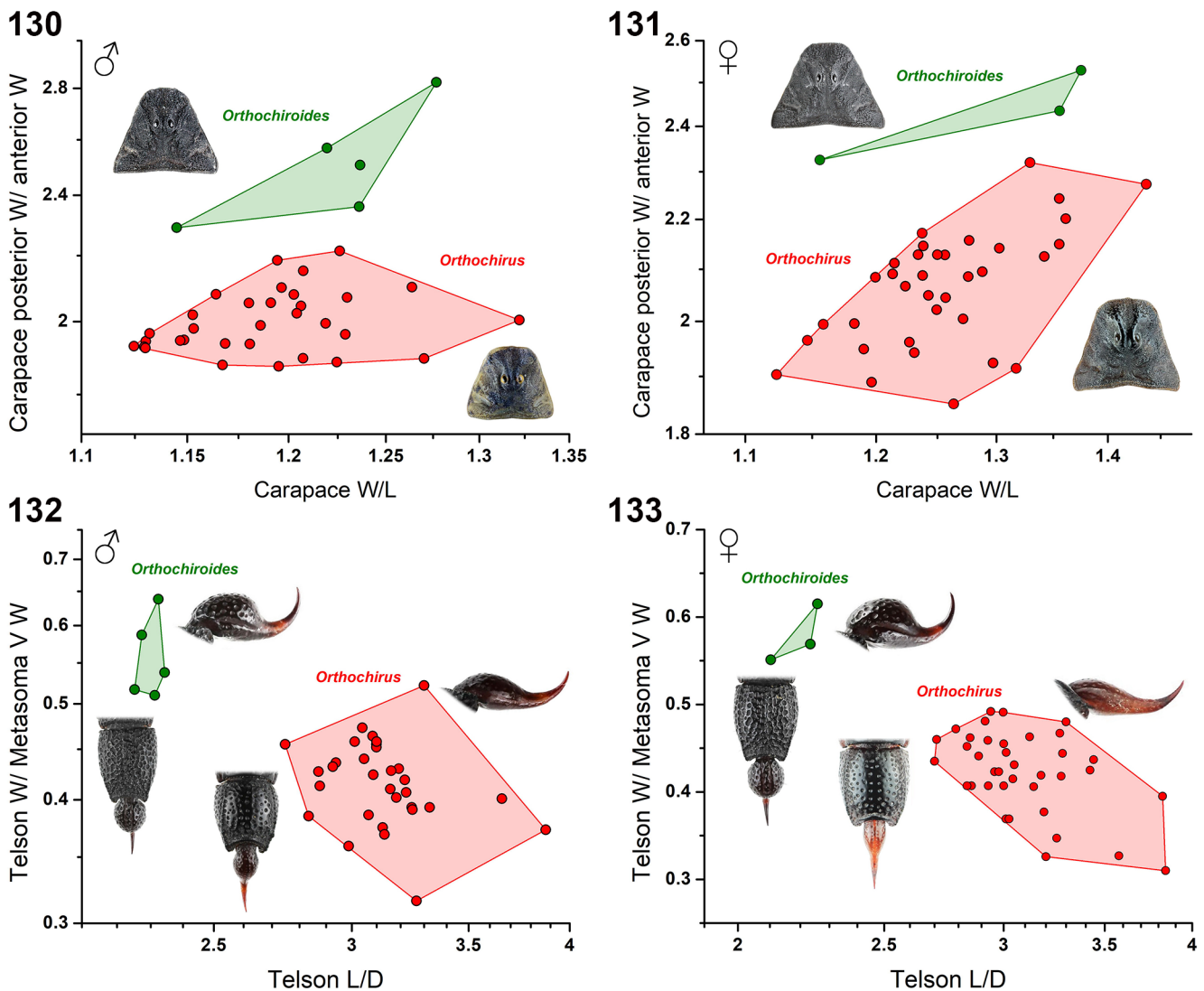
Figures 130–133: Comparative morphometrics of carapace, metasoma V and telson of *Orthochiroides* and *Orthochirus*. **Figures 130–131**. Bivariate scatter plots of the ratios of carapace posterior W/ carapace anterior W vs. carapace posterior W/ carapace L for males (130) and females (131). Illustrated species: *Orthochiroides somalilandus* **sp. n.** (♂♀), *Orthochirus olivaceus* (♂), *Orthochirus masihipouri* (♀). Sample: *Orthochiroides*: 4 spp. (♂♀); *Orthochirus*: 32 spp. (♂), 35 spp. (♀). **Figures 132–133**. Bivariate scatter plots of the ratios of telson W/ metasoma V W vs. telson L/ telson D for males (132) and females (133). Illustrated species: *Orthochiroides somalilandus* **sp. n.** (♂♀), *Orthochirus semnanensis* (♂), *Orthochirus birulai* (♀). Sample: *Orthochiroides*: 4 spp. (♂), 3 spp. (♀); *Orthochirus*: 32 spp. (♂), 39 spp. (♀). Ratios linearized by logarithmic axes. Carapace anterior W measured as distance between the most anterior pair of lateral ocelli.

Orthochirus (39 spp., 73% of named species). The distribution of the ratio was widely disjunct between *Orthochiroides* and *Orthochirus*, with consistently higher values in the latter for both sexes. Two additional morphometric trends may distinguish the two genera: the bulbous telson of *Orthochiroides* is typically wider than that of *Orthochirus*, and the posterior metasomal segments of *Orthochirus* exhibit greater lateral expansion compared to those of *Orthochiroides*. We analyzed the ratio of telson W/ metasoma V W, and found it to be invariably larger for female *Orthochiroides*, and mostly larger for males (overlapping for only one species of *Orthochirus*). Bivariate scatter plots of the two ratios revealed the wide disjunction between the two genera in 2D morphospace (Figs. 132–133). See also Figs. 120–121 vs. figs. 122–123.

Lourenço & Ythier (2021: 339) rejected telson shape as a diagnostic character for *Orthochiroides* because "*many other genera have strong variations in the shape of the telson*". However, their vague claim was devoid of any support from actual data or analyses. We previously analyzed the telson shapes of a large sample of taxa of Order Scorpiones (Lowe et al., 2019). Here, we test their claim by extending that analysis to include *Orthochiroides* and a majority (85%) of named species of *Orthochirus*. Telson lateral profiles were parametrized by measuring 7 biometric variables (Fig. 136), normalized to telson length. Data were extracted from 2,562 distinct profiles (in total 20,496 measurements; 52.3% ♂, 47.7% ♀) representing 20 families, 224 genera and 1,866 species (70.18% of all currently named species, Rein (2022),
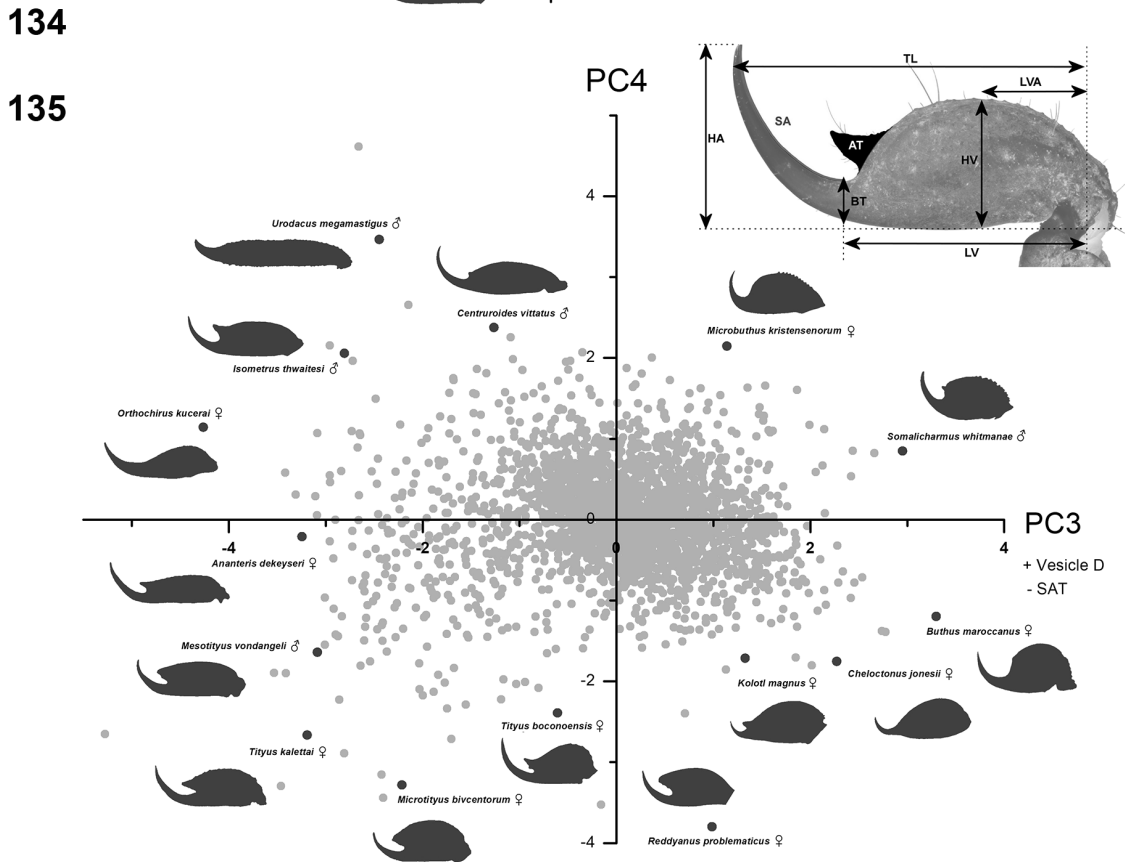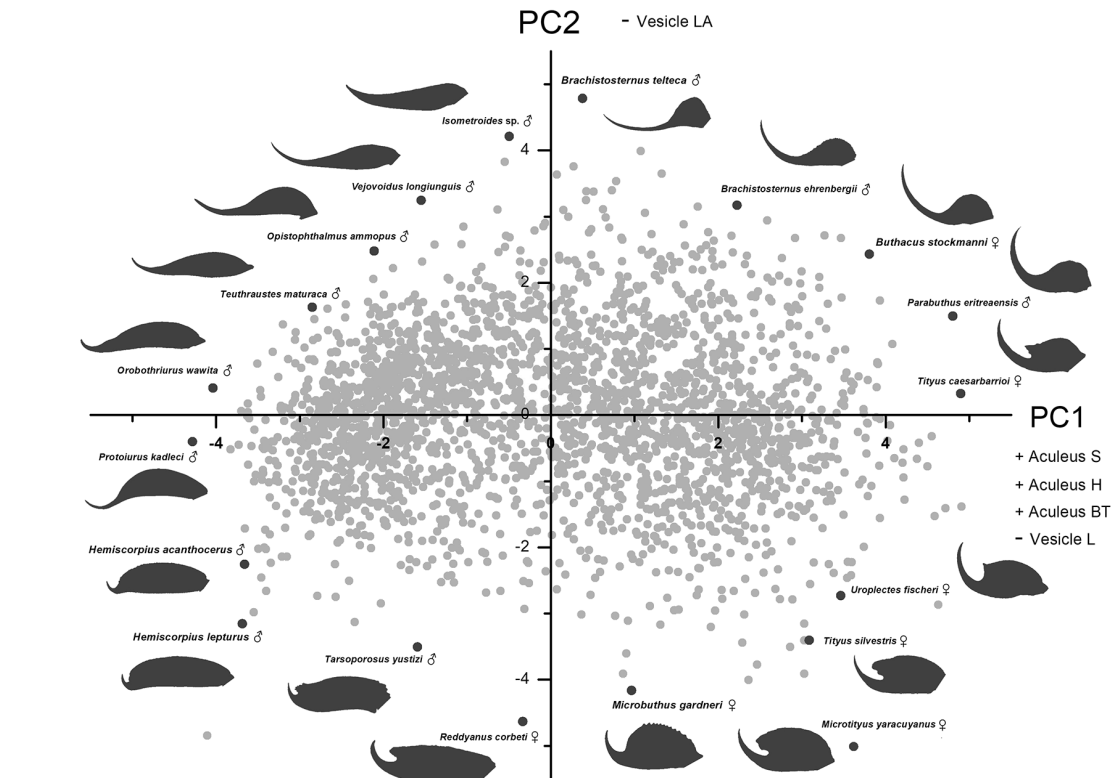
Figures 134–135: Morphometric analysis of scorpion telson shape. Bivariate scatter plots of principal component scores, PC1 vs. PC2 (134) and PC3 vs. PC4 (135) explaining 94.36% of the variance of telson lateral profiles parametrized by 7 variables (136): LV (vesicle length), LVA (anterior vesicle length), HV (vesicle depth), HA (aculeus height), SA (aculeus ventral curve length), BT (aculeus basal thickness), and AT (area of subaculear tubercle). First 6 variables normalized to telson length (TL), AT normalized to area of vesicle bounding box (LV.HV). Axis labels list associated variables with factor loadings > 50% (positive or negative). Sample: 2562 profiles; families: 20; genera, 224; species, 1866 (1858 extant, 8 extinct); sex, 1340 ♂ + 1213 ♀ + 9 ?. Data compilation as in Lowe et al, 2019.
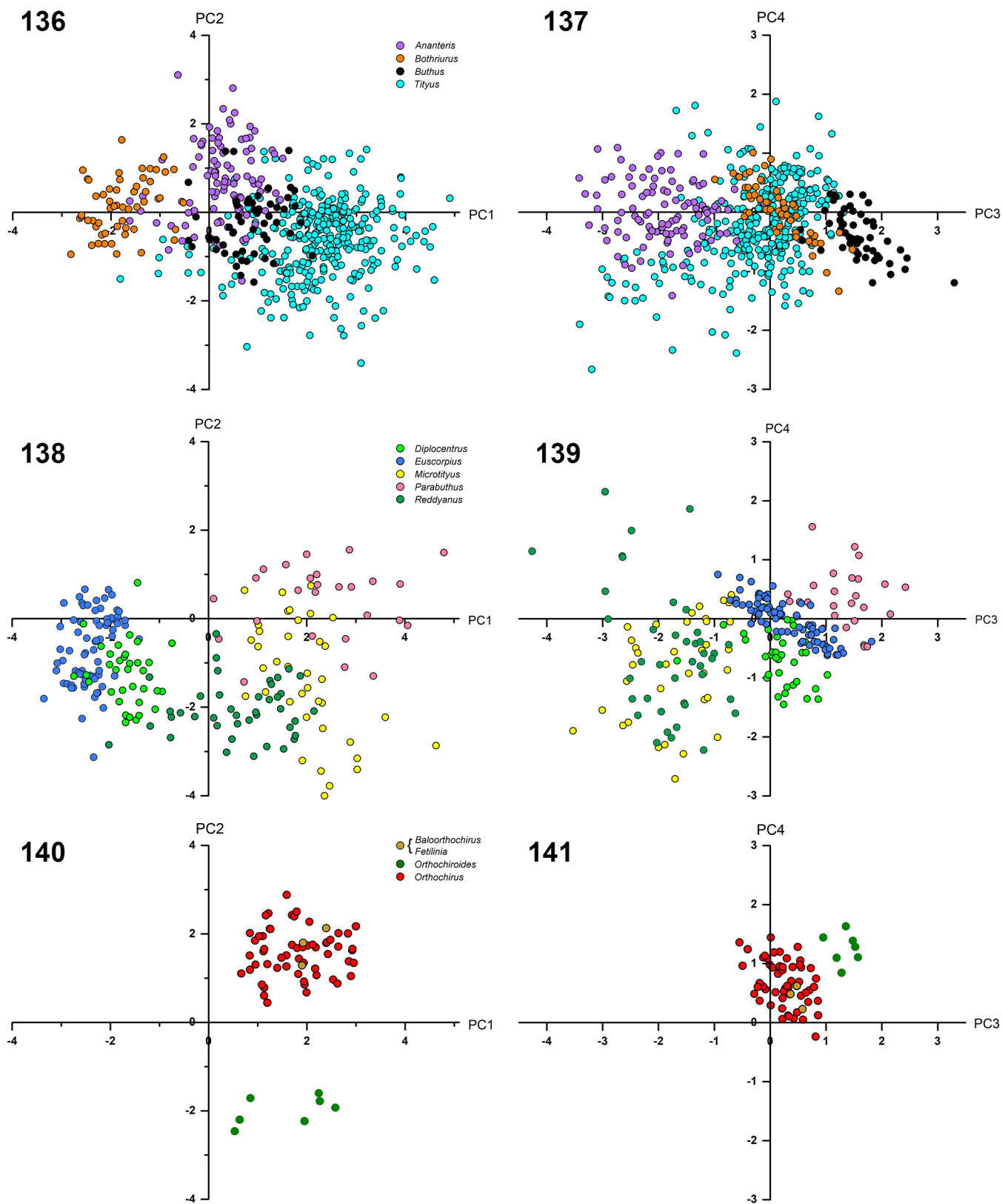
Figures 136–141: Variation in telson shape of scorpion genera. Bivariate scatter plots of principal component scores, PC1 vs. PC2 (136, 138, 140) and PC3 vs. PC4 (137, 139, 141) for selected genera: *Ananteris* (83 spp.), *Bothriurus* (35 spp.), *Buthus* (43 spp.) and *Tityus* (199 spp.) (136–137); *Diplocentrus* (32 sp.), *Euscorpius* (43 spp.), *Microtityus* (32 sp.), *Parabuthus* (22 sp.) and *Reddyanus* (27 spp.) (138–139); *Baloorthochirus* (1 sp.), *Fetilinia* (1 sp.), *Orthochiroides* (4 spp.) and *Orthochirus* (43 spp.) (140–141).

Figures 142–165: Ventral profiles of metasoma and telson of male *Orthochiroides* and *Orthochirus*. **Figures 142–146**. *Orthochiroides insularis* (142), *O. socotrensis* (143), *O. vachoni* (143–145), *O. somalilandus* (146), *Orthochirus socotrensis* (143). **Figures 147–165**. *Orthochirus afar* (147), *O. fomichevi* (148), *O. formozovi* (149), *O. gantenbeini* (150), *O. hormozganensis* (151), *O. iranus* (152), *O. iraqus* (153), *O. kermanensis* (154), *O. kryzhanovskyi* (155), *O. kucerai* (156), *O. melanurus* (157), *O. mesopotamicus* (158), *O. nordmanni* (159), *O. olivaceus* (160), *O. persa* (161), *O. semnanensis* (162), *O. stockwelli* (163), *O. vignolii* (164), *O. zagrosensis* (165). Colored arrows: character 29, antero-lateral corners of metasoma IV (green = flush, 0; blue = wedge-shaped, 1); character 32, widening of metasoma III near posterior margin (orange = graded, 0; red = abrupt, 1). Figs. 147–165 after: Kovařík et al., 2016, 2019b, 2020a, 2020b; Kovařík & Navidpour, 2020; Navidpour et al., 2019.

Figures 166–188: Ventral profiles of metasoma and telson of female *Orthochiroides* and *Orthochirus*. **Figures 166–167**. *Orthochiroides insularis* (166), *O. somalilandus* (167). **Figures 168–188**. *Orthochirus afar* (168), *O. birulai* (169), *O. carinatus* (170), *O. fomichevi* (171), *O. formozovi* (172), *O. grosseri* (173), *O. gruberi* (174), *O. hormozgonensis* (175), *O. iranus* (176), *O. kermanensis* (177), *O. kucerai* (178), *O. masihipouri* (179), *O. melanurus* (180), *O. mesopotamicus* (181), *O. navidpouri* (182), *O. nordmanni* (183), *O. olivaceus* (184), *O. persa* (185), *O. scrobiculosus* (186), *O. sejnai* (187), *O. vignolii* (188). Colored arrows: character 29, antero-lateral corners of metasoma IV (green = flush, 0; blue = wedge-shaped, 1); character 32, widening of metasoma III near posterior margin (orange = graded, 0; red = abrupt, 1). Figs. 168–188 after: Kovařík et al., 2016, 2019b, 2020a, 2020b; Kovařík & Navidpour, 2020; Navidpour et al., 2019.
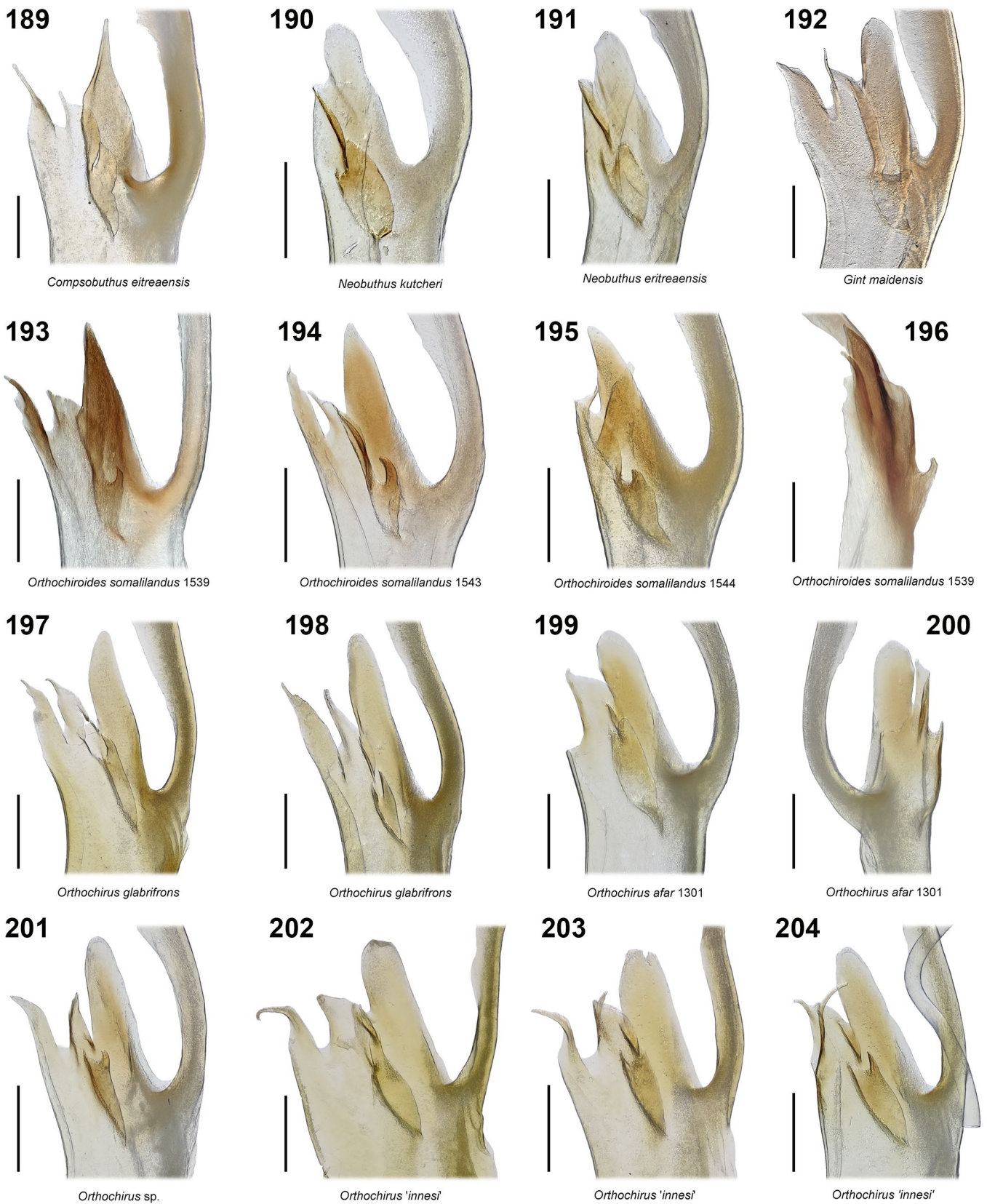
Figures 189–204: Hemispermatophore capsules of *Compsobuthus*, *Neobuthus*, *Gint*, *Orthochiroides* and *Orthochirus*. **Figure 189**. *Compsobuthus eritreaensis*. **Figures 190–191**. *Neobuthus kutcheri* (190), *N. eritreaensis* (191). **Figure 192**. *Gint maidensis*. **Figures 193–196**. *Orthochiroides somalilandus*, DNA specimens 1539, 1543, 1544. **Figures 197–204**. *Orthochirus glabrifrons* (197–198), *O. afar*, DNA specimen 1301 (199–200), *O.* sp., Morocco, DNA specimen 1165 (201), *O.* 'innesi', Oman (202–204). Convex (189–195, 197–199, 201–204), anterior (196) and posterior (200) views. Convex views show compressed profiles. Scale bars: 200 μm.
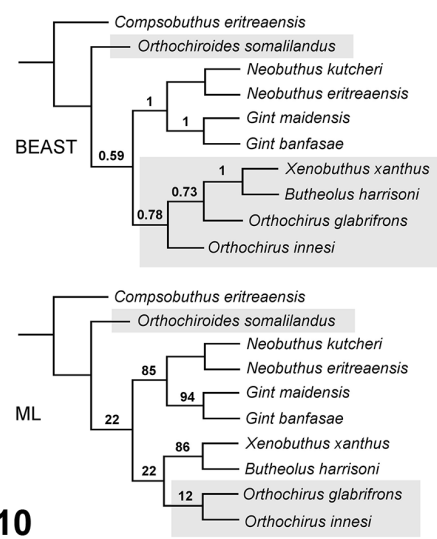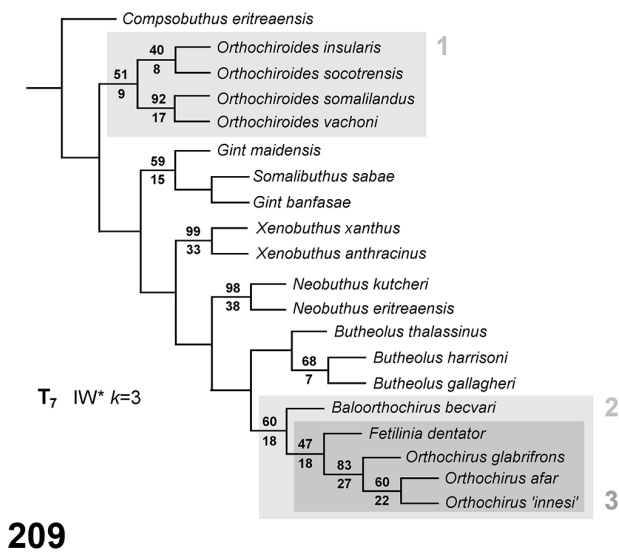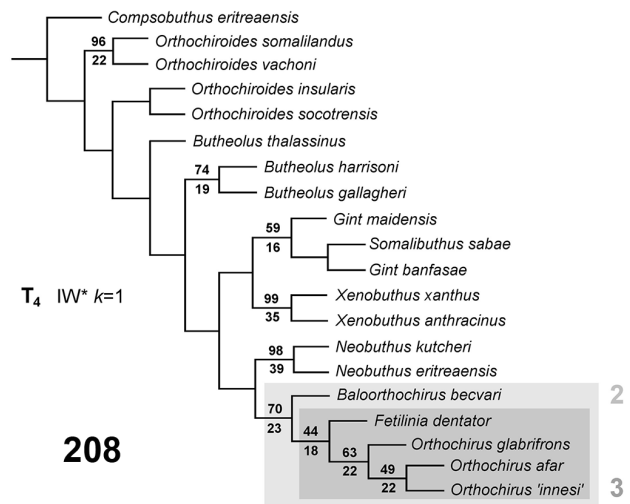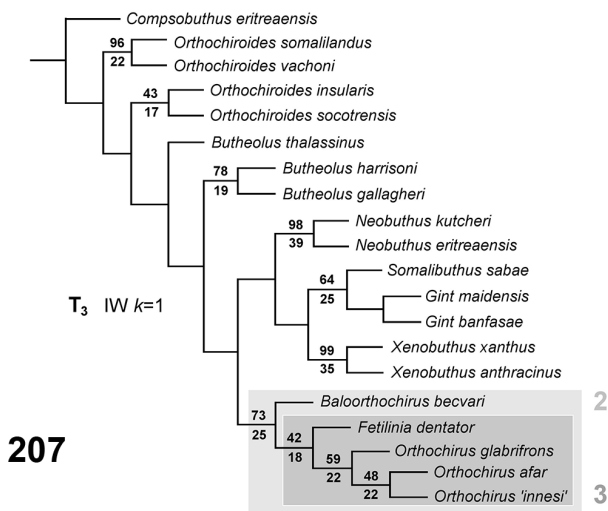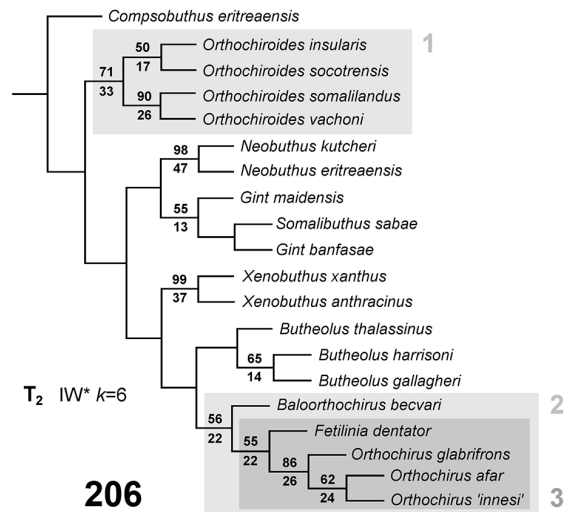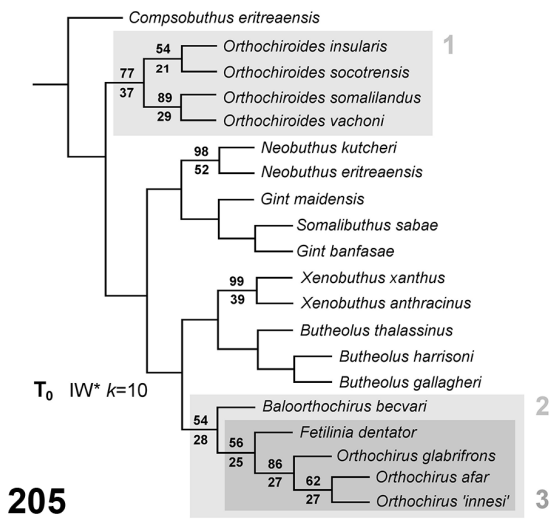
Figures 205–210: Phylogenetic analysis of *Orthochiroides*, and *Orthochirus* and related buthid genera. **Figures 205–209**. Examples of most parsimonious trees (T_0, T_2, T_3, T_4 and T_7) retrieved by cladistic analyses of 43 morphological characters under equal and implied weights. Numbers above indicate jackknife supports (36% resampling probability), those below relative Bremer supports, computed for implied weights (IW), concavity constant $k = 1$ (207), and implied weights with characters 1 and 2 irreversible (IW*), concavity constants $k = 10$ (205), $k = 6$ (206), $k = 1$ (208) and $k = 3$ (209). Gray panels 1, 2 and 3: clades of interest. **Figure 210**. Phylogenetic trees of a subset of the exemplar species in Figs. 205–209, reconstructed by Bayesian inference (BEAST) and maximum likelihood (ML) analyses of multilocus sequence data (Štundlová et al., 2022) (node supports indicated).
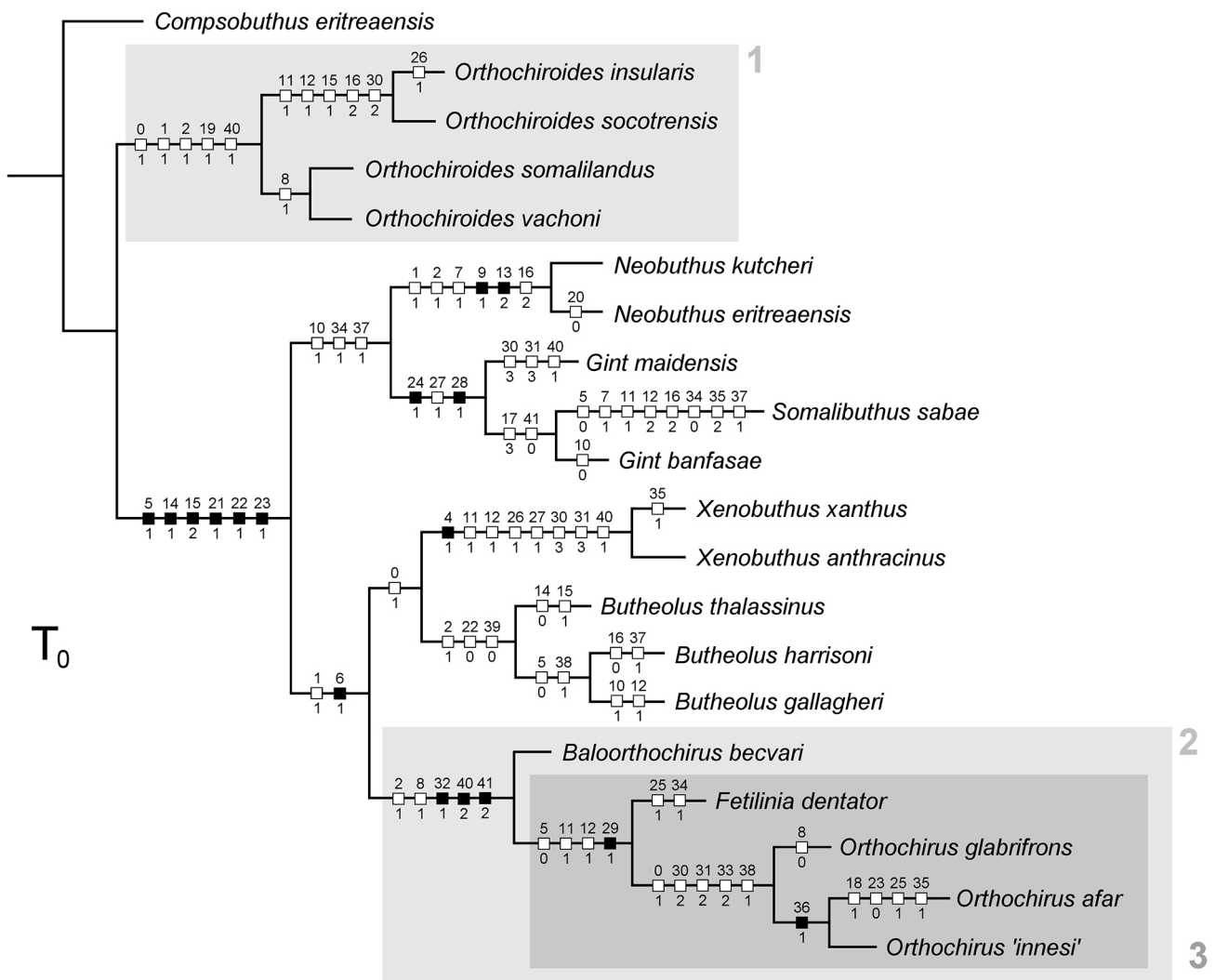
Figure 211: Phylogenetic tree with topology T$_0$, retrieved by cladistic analyses of 43 morphological characters under equal weights and implied weights with concavity constants $k = 10 – 30$ (IW), and $k = 4 – 30$ (IW*). Boxes indicate unambiguous synapomorphies, filled boxes unique (derived once with reversals allowed), open boxes homoplasious synapomorphies (derived more than once). Numbers above nodes are character identifiers, those below nodes character states. Gray panels 1, 2 and 3: clades of interest.

a statistically significant sample). Principal components analysis reduced the dimensions to 4 variables (PC1–PC4) explaining a cumulative 94.36% of the variance (eigenvalues: 3.7509, 1.4463, 0.9487, 0.4590; respective variances: 53.58%, 20.66%, 13.55%, 6.56%). On the basis of > 50% loading of variables on principal components, we interpreted PC1 as related positively to aculeus length, height and thickness, and negatively to vesicle length, PC2 negatively to vesicle anterior length, and PC3 positively to vesicle depth, and negatively to subacular tubercle size (Table 2). The distribution of scores for the entire order is shown in bivariate scatter plots of PC1 vs. PC2 (Fig. 134) and PC3 vs. PC4 (Fig. 135). In Figs. 136–139, scores for 9 selected genera are mapped in these 2D subspaces of the 4D reduced morphospace. It is evident that each genus is distributed within a specific domain of morphospace, corresponding to its range of expressed telson shapes. Domains of different genera may be broadly overlapped,

reflecting similarities of shapes among the various genera. Some genera are spread over larger domains, while others are restricted to smaller domains. The former may indeed be characterized as having "*strong variations in the shape of the telson*". For example, the speciose New World buthid genus *Tityus* is widely distributed in telson morphospace, although it has been proposed to be divided into subgenera (Lourenço, 2006) and it remains to be seen if future studies will justify splitting it into more than one genus.

The diagnosis of *Orthochiroides* as a genus distinct from *Orthochirus* is, however, based not merely on a difference in telson shapes, but specifically on the distribution of their shapes in morphospace. Figs. 140–141 show the distributions of principal components scores of these two genera. If *Orthochiroides* were a synonym of *Orthochirus*, then this single genus would exhibit a split distribution of two widely separated clusters in PC1-PC2 subspace (Fig. 140, red vs. green

	PC1	PC2	PC3	PC4	PC5	PC6	PC7
LV	-0.853037	-0.399430	0.075317	-0.000461	0.262549	0.192319	0.034532
HV	0.370376	-0.515146	0.691653	-0.333706	-0.084030	-0.025187	0.002567
LVA	-0.096101	-0.897091	-0.166714	0.352007	-0.179072	-0.047140	-0.000780
AT	0.495406	-0.398100	-0.651368	-0.412205	0.042877	0.007587	-0.000264
HA	0.956130	-0.074702	0.071292	0.134592	0.048030	0.228323	-0.050983
SA	0.962140	0.172893	-0.027646	0.086333	-0.147602	0.097235	0.070252
BT	0.889642	-0.150447	0.082259	0.168032	0.351520	-0.164971	0.010922

Table. **2**. Factor loadings of principal components extracted from seven biometric variables quantifying telson shape. See Figs. 134–135 for variable abbreviations.

Taxon	0–4	5–9	10–14	15–19	20–24	25–29	30–34	35–39	40–42
Compsobuthus eritreaensis	00000	00000	00000	00000	00000	00000	00000	00000	000
Orthochiroides vachoni	11100	02010	00010	00?11	00000	00000	01010	10021	110
Orthochiroides somalilandus	11100	02010	00010	00011	00000	00000	01010	10021	110
Orthochiroides socotrensis	11100	02000	01110	12?11	10000	00000	22020	10011	110
Orthochiroides insularis	11100	02000	01110	12?01	10000	1000	22020	10011	110
Neobuthus eritreaensis	01100	12101	10021	22000	01110	00000	00001	00101	010
Neobuthus kutcheri	01100	12101	10021	22000	11110	00000	00001	10101	010
Gint banfasae	00000	10000	00011	20300	11111	00110	00001	10101	000
Gint maidensis	00000	10000	10011	20000	11111	00110	33001	10101	110
Somalibuthus sabae	00000	00100	11211	22300	11111	00110	00000	20001	000
Xenobuthus anthracinus	11011	11000	01111	21301	11110	01100	33000	00001	110
Xenobuthus xanthus	11011	11000	01111	21301	11110	01100	33000	10001	110
Butheolus gallagheri	11110	01000	10111	21102	11010	00000	00000	00010	010
Butheolus harrisoni	11110	01000	00011	20102	11010	00000	00000	00110	010
Butheolus thalassinus	11100	11000	00010	11?02	11010	00000	00000	00000	010
Baloorthochirus becvari	01100	11010	00011	20?00	11110	00000	00100	00001	221
Fetilinia dentator	01110	01010	01111	21?00	11110	10001	00101	00001	220
Orthochirus glabrifrons	11110	01000	01111	20200	11110	00001	22120	00011	221
Orthochirus innesi	11110	01010	01111	21200	11110	00001	22120	01011	221
Orthochirus afar	11110	01010	01111	21210	11100	10001	22120	11011	221

Table. **3**. Character matrix for phylogenetic analysis of *Orthochiroides* and exemplar species of *Orthochirus* and similar buthid genera. Numbered characters as defined in the Table 3.

symbols). The disjunct distribution mirrors that of Figs. 132–133. On the other hand, the wide variations in telson shapes of other genera (Figs. 136–139) were not clearly segregated into discrete clusters, but were more or less continuously dispersed with intermediate forms linking the varied shapes. This was not the case for *Orthochiroides* and *Orthochirus*, which lack any intermediate forms between the bulbous shape of the former, and the slender shape of the latter. We mapped morphospace distributions of 97 other scorpion genera, each represented by samples of more than 4 data points, and found none with a similarly conspicuous separation into two or more clusters. A potential clustering into two groups was only seen in *Uroplectes* Peters, 1861, a genus that has not been revised recently and whose monophyly is untested. A small minority of species with telson shapes that are highly divergent from those of their congeners seem to be isolated cases that have

evolved specialized autapomorphies, e.g., *Urodacus mckenziei* Volschenk et al, 2000, *U. megamastigus* L. E. Koch, 1977, and *Chaerilus pictus* (Pocock, 1890). Synonymy of *Orthochiroides* with *Orthochirus* would manufacture a genus with two highly divergent telson shapes, a property that is absent in almost all other currently recognized scorpion genera. Maintaining them as distinct genera complies with the prevalent taxonomic convention.

(iii) Metasoma III–IV, **anterior corners**: *Orthochiroides*: corners flush with anterior margin, or almost so, not projecting forward and outward; *Orthochirus*: corners wedge-shaped, projecting forward and outward (♂♀) (character 29, states 0 and 1).

In ventral profile, the anterior corners of metasoma III–IV in *Orthochiroides* are level with, or extend only slightly

Weights	N_{MPT}	MPTs	Steps	AH	CI	RI	$\bar{J}$	J1	J2	J3
EW	2	T_0, T_1	119	–	0.496	0.704	50.9	44	16	52
IW k = 1	1	T_3	122	19.1905	0.484	0.690	58.1	–	71	46
IW k = 2	1	T_5	122	14.3976	0.484	0.690	57.1	–	65	46
IW k = 3	1	T_3	122	11.5917	0.484	0.690	54.8	–	60	48
IW k = 4	1	T_6	122	9.7270	0.484	0.690	55.5	–	55	51
IW k = 5	1	T_8	121	8.3788	0.488	0.695	55.9	–	51	51
IW k = 6	1	T_8	121	7.3593	0.488	0.695	55.9	–	47	55
IW k = 8	1	T_9	120	5.9134	0.492	0.700	56.4	28	42	59
IW k = 10	1	T_0	119	4.9326	0.496	0.704	56.1	30	39	59
IW k = 15	1	T_0	119	3.4899	0.496	0.704	56.0	33	37	60
IW k = 30	1	T_0	119	1.8619	0.496	0.704	56.0	35	35	59
EW*	2	T_0, T_2	121	–	0.488	0.722	48.8	78	35	50
IW* k = 1	2	T_4, T_5	130, 129	19.8238	0.454, 0.457	0.682, 0.686	50.5	–	69	44
IW* k = 2	1	T_5	133	15.1119	0.457	0.686	47.9	–	62	45
IW* k = 3	1	T_7	122	12.1464	0.484	0.717	49.3	51	60	47
IW* k = 4	1	T_0	121	10.1032	0.488	0.722	51.0	62	58	51
IW* k = 5	2	T_0, T_2	121	8.6587	0.488	0.722	51.7	68	57	52
IW* k = 6	2	T_0, T_2	121	7.5807	0.488	0.722	52.1	71	56	55
IW* k = 8	1	T_0	121	6.0755	0.488	0.722	52.8	75	53	56
IW* k = 10	1	T_0	121	5.0724	0.488	0.722	53.0	77	53	56
IW* k = 15	1	T_0	121	3.5941	0.488	0.722	53.1	78	51	56
IW* k = 30	1	T_0	121	1.9205	0.488	0.722	53.2	79	51	56

Table. 4. Statistics of most parsimonious trees (MPTs) retrieved by cladistic analysis of the character matrix in Table 3, rooted by outgroup taxon *Compsobuthus eritreaensis*. **Weights**: different weighting schemes tested; **EW/ IW**: equal weights/ implied weights, all characters reversible; **EW*/ IW***: equal weights/ implied weights, characters 1 & 2 irreversible; **k**, concavity constant for implied weighting; N_{MPT}: number of MPTs; **MPTs**: list of MPTs retrieved under each weighting scheme: T_i, i = 0–9; **Steps**: tree length in total number of character transformation steps; **AH**: adjusted homoplasy (for implied weights); **CI**: tree consistency index; **RI**: tree retention index; $\bar{J}$: average jackknife support from 4,000 pseudoreplicates, 36% resampling probability; J_i, i = 1–3: node support for clades 1–3 indicated by the shaded panels in Figs. 205–209, 211; **J1**: ((*Orthochiroides insularis*, *O. socotranus*), (*O. somalilandus*, *O. vachoni*)); **J2**: (*Baloorthochirus becvari*, (*Fetilinia dentator*, (*Orthochirus glabrifrons*, (*O. afar*, *O.* 'innesi')))); **J3**: (*Fetilinia dentator*, (*Orthochirus glabrifrons*, (*O. afar*, *O.* 'innesi'))). Gray cells indicate **J1**, **J2** or **J3** support > 50%, blank cells indicate clade for **J1** was not recovered.

forward from the antero-ventral margin, and not outward (Figs. 142–146, 166–167; green arrows, character state 0). In contrast, the anterior corners of metasoma III–IV in *Orthochirus* extend distinctly forward and outward from the antero-ventral margin as wedge-shaped processes (Figs. 147–165, 168–188; blue arrows, character state 1).

(iv) Metasoma II–III, **posterior width**: *Orthochiroides*: widening gradually from posterior margin; *Orthochirus*: widening abruptly from posterior margin (♂♀) (character 33, states 0 and 1).

In ventral profiles, the posterior ends of metasoma II–III in *Orthochiroides* gradually widen with increasing forward distance from the posterior margin (Figs. 142–146, 166–167; orange arrows, character state 0). In contrast, the posterior ends of metasoma II–III in *Orthochirus* are abruptly widened. A narrower annulus at the posterior margin connects to a widely flared section in front of it (Figs. 147–165, 168–188; red arrows, character state 1). This leaves a gap or recess at each posterior corner to accommodate the anterior corner

wedge of the next segment. The different, more specialized construction in *Orthochirus* allows consecutive segments to be more tightly interlocked when the metasoma is folded or coiled.

(v) Sternite VI, **submedian carinae**: *Orthochiroides*: distinct, granulate to weakly crenulate; *Orthochirus*: indistinct, smooth to obsolete (♂♀) (character 21, states 0 and 1) (cf. Kovařík, 1998: 116: *Orthochiroides*, "*mesosoma with one dorsal and four ventral keels*").

(vi) Sternites III–VII, **posterior margins**: *Orthochiroides*: coarsely denticulate, armed with fringes of non-contiguous, enlarged blunt denticles; *Orthochirus*: finely microdenticulate or smooth (♂♀) (character 19, states 1, 2 and 0).

The sternite posterior margins in *Orthochirus* are similar to those of most other buthids, in being either smooth or bearing very fine, triangular microdenticles that are densely spaced, separated from each other by less than their widths. The sternite marginal denticles in *Orthochiroides* are much

	Character	Steps	CI	RI
0	Base color: lighter, yellow to light brown (0); darker, dark brown to black (1).	3	0.333	0.714
1	Carapace, antero-submedian carinae: strong, granulate (0); reduced or obsolete (1).	3	0.333	0.867
2	Carapace, central median carinae: strong (0); reduced or obsolete (1).	4	0.250	0.769
3	Carapace, superciliary carinae, ♂: granulate (0); smooth (1).	3	0.333	0.714
4	Carapace granulation density: dense (0); sparse (1).	1	1.000	1.000
5	Carapace, granulation size: fine (0); coarse (1).	4	0.250	0.571
6	Carapace shape: subrectangular (0); moderately trapezoidal (1); strongly trapezoidal (2).	3	0.667	0.875
7	Cheliceral fixed finger, ventral accessory denticles: 2 (0); 1 (1).	2	0.500	0.500
8	Pedipalp femur, petite 'trichobothrium' d_2 on dorsal surface: present (0); absent (1).	3	0.333	0.600
9	Pedipalp femur, trichobothrium e_1 position: proximal (0), submedian (1).	1	1.000	1.000
10	Pedipalp patella, dorsomedian carina, ♂: complete (0); incomplete (1).	3	0.333	0.500
11	Pedipalp patella, dorsomedian carina, ♂: granulate (0); smooth (1).	4	0.250	0.625
12	Pedipalp patella, dorsoexternal carina, ♂: granulate (0); smooth (1); absent (2).	5	0.400	0.625
13	Pedipalp chela manus, trichobothrium V_2 position: external (0); medial (1); internal (2).	2	1.000	1.000
14	Pedipalp chela manus V1, VA, D3 carinae: strong (0); weak or obsolete (1).	2	0.500	0.800
15	Pedipalp chela manus E carina: strong (0); weak (1); obsolete (2).	3	0.667	0.750
16	Pedipalp chela fixed finger trichobothrium dt vs. et: distal (0); level (1); proximal (2).	7	0.286	0.500
17	Hemispermatophore basal lobe: broad hook (0); narrow hook (1); laminate hook (2); scoop (3).	4	0.750	0.833
18	Tergite V-VI carination: tricarinate (0); obsolete (1).	3	0.333	0.333
19	Sternite III-V posterior marginal denticles: small (0); enlarged, ♂ = ♀ (1); enlarged, ♂ > ♀ (2).	3	0.667	0.857
20	Sternite V antero-medial fine granulation, ♂: present (0); absent (1).	3	0.333	0.333
21	Sternite VI submedian carinae: distinct (0); obsolete (1).	1	1.000	1.000
22	Sternite VI lateral carinae, ♂: distinct (0); obsolete (1).	2	0.500	0.857
23	Sternite VI antero-medial surface texture: matte (0); glossy (1).	2	0.500	0.800
24	Sternite VII submedian carinae: present (0); absent (1).	1	1.000	1.000
25	Sternite VII lateral carinae: present (0); absent (1).	2	0.500	0.000
26	Metasoma I dorsal granulation, ♂: present (0); absent (1).	2	0.500	0.500
27	Metasoma I ventromedial surface: granulate (0); smooth (1).	2	0.500	0.750
28	Metasoma I ventrosubmedian carinae: strong (0); weak/ obsolete (1).	1	1.000	1.000
29	Metasoma III-IV, anterior corners: flush (0); wedge-shaped processes (1).	1	1.000	1.000
30	Metasoma II, lateral surface: granulate (0); rugose-reticulate (1); punctate (2); smooth (3).	4	0.500	0.667
31	Metasoma III, lateral surface: granulate (0); rugose-reticulate (1); punctate (2); smooth (3).	5	0.600	0.714
32	Metasoma III, widening from posterior margin: continuous (0); abruptly stepped (1).	1	1.000	1.000
33	Metasoma V, ventromedian surface: granulate (0); rugose-reticulate (1); punctate (2).	3	0.667	0.800
34	Metasoma V ventrolateral carinae: granulate (0); lobate (1).	3	0.333	0.500
35	Metasoma V dorsosubmedian carinae: granulate (0); smooth (1); obsolete (2).	6	0.333	0.500
36	Metasoma segment V vs. I width increase: < 10% (0); > 10% (1).	1	1.000	1.000
37	Metasomal macrosetae, length: ♂ = ♀ (0); ♂ < ♀ (1).	3	0.333	0.500
38	Telson vesicle ventral surface, punctation: absent (0); weak (1); strong (2).	4	0.500	0.714
39	Telson vesicle ventral surface, granulation: moderate to strong (0); weak or absent (1) .	2	0.500	0.667
40	Telson vesicle lateral profile, ♂: hemi-elliptic (0); bulbous (1); slender, pyriform (2).	4	0.500	0.800
41	Telson vesicle posterior slope: moderate (0); steep (1); shallow (2).	3	0.667	0.833
42	Telson vesicle W/ metasoma V W: > 0.5 (0); < 0.5 (1).	2	0.500	0.667

Table. 5. Lengths (**Steps**), consistency indices (**CI**) and retention indices (**RI**) of individual characters mapped to the most parsimonious tree, T_0 (EW).

larger, blunt, clavate or digitate in shape, and are well separated from each other by more than their widths. Similar enlarged marginal denticles are also found on the sternites of *Butheolus* and *Xenobuthus*, and serve as a diagnostic character at the genus level, e.g., to separate *Butheolus* and *Xenobuthus* from *Neobuthus* (Kovařík & Lowe, 2012; Lowe, 2018). In *Butheolus*, the enlarged denticles are sexually dimorphic, with males bearing larger denticles than females. In *Orthochiroides* and *Xenobuthus*, the enlarged denticles are of the same size in both sexes.

(vii) Pedipalp chela manus, **carinae**: *Orthochiroides*: carinae V1, VA, D3 strong and costate, E either strong and costate, or weak; *Orthochirus*: carinae V1, VA, D3 weak, E obsolete

(♂♀) (character 14, states 0 and 1; character 15, states 0/1 and 2) (cf. Kovařík, 1998: 116: *Orthochiroides*, "*six pronounced keels on the tibia of pedipalps*").

The ventroexternal (V1), ventral accessory (VA) and dorsal secondary (D3) carinae are strongly developed in all four species of *Orthochiroides* (Figs. 19–21, 28–30, 64–66, 87–88, 91–92, 95–96, 99–100, 103–104, 107–108). The external secondary carina (E) is strongly developed in *Orthochiroides vachoni* and *O. somalilandus* **sp. n.** (Figs. 19–21, 28–30, 64–66, 103–104, 107–108), and weakly developed in *O. insularis* and *O. socotrensis* (Figs. 87–89, 91–92, 95–96, 99–100). In *Orthochirus*, these carinae on the manus are attenuated, either reduced to weak, smooth carinae (V1, VA, D3) or obsolete (E).

Phylogenetic analysis of *Orthochiroides* Kovařík, 1998 vs. *Orthochirus* Karsch, 1891

The proposed synonymy of *Orthochiroides* with *Orthochirus* by Lourenço & Ythier (2021: 339) equates to the hypothesis that these two genera together comprise a monophyletic group. To test this hypothesis, we conducted a cladistic analysis of an ingroup that included all species of *Orthochiroides*, plus selected exemplar species representing *Orthochirus* and other morphologically similar genera of small buthids (*Neobuthus* Hirst, 1911, *Gint* Kovařík et al, 2013, *Butheolus* Simon, 1882, *Xenobuthus* Lowe, 2018, *Baloorthochirus* Kovařík, 1996 and *Fetilinia* Lowe & Kovařík, 2021; Table 3). As outgroup taxon we selected *Compsobuthus eritreaensis* Kovařík, Lowe, Plíšková & Šťáhlavský, 2016. This selection was guided by results of a molecular phylogenetic study in which this species, along with other *Compsobuthus* species, was placed in the immediate sister clade of a larger clade including all of our DNA-sampled ingroup taxa (Štundlová et al., 2022). We analyzed a matrix of 43 discrete morphological characters (Tables 3, 5) These characters were selected on the basis of: (i) their relative intrageneric stability for ingroup taxa, with most having minor or no interspecific variation within each genus; and (ii) their systematic variation across genera of the ingroup, which was potentially informative about higher level relationships. They included 25 binary characters and 18 unordered multistate characters. Phylogenetically uninformative characters were excluded from the analyses. Two binary characters (characters 1 and 2: loss of antero-submedian and central median carinae on the carapace) were tested under assumptions of both reversibility and irreversibility. Intrageneric stability ensured that results about intergeneric relationships would not be sensitive to our representation of the larger genera (*Neobuthus* and *Orthochirus*) by a minority of their named species. Additional exemplars of these genera would have identical, or almost identical, character scores as those already included, and are therefore expected to only introduce polytomies at their respective genus nodes.

We conducted 22 analyses, assuming either equal weights, or implied weights with varying strengths of concavity (k = 1–6, 8, 10, 15, 30). In total, nine distinct most parsimonious trees (T_i, i = 0–8) were retrieved (Table 4). A monophyletic including all species of *Orthochiroides*, clade 1 = ((*Orthochiroides insularis*, *O. socotrensis*), (*O. somalilandus*, *O. vachoni*)), was resolved in 14/22 analyses. Clade 1 was separated from, and basal to, other ingroup taxa. It received significant support in 9/11 analyses that assumed irreversibility of characters 1 and 2 (e.g., upper gray panels in Figs. 205–206, 209). If reversibility was permitted, the carapace carinae were initially lost for the entire ingroup and later regained in *Gint*, *Somalibuthus* and *Xenobuthus*. Irreversibility assumes that once lost, a compound structure like a carina is less likely to be reconstructed de novo in these genera, which also possess other plesiomorphic characters, than it is to be lost independently in the more specialized lineages (clades 1, 2

and 3), which also possess other apomorphic characters. In most cases, imposing irreversibility had little effect on tree lengths, but increased support for clade 1 (*Orthochiroides*) which gained two synapomorphies (i.e., carinal losses).

In all of the analyses and tree topologies, either clade 2 = (*Baloorthochirus becvari*, (*Fetilinia dentator*, (*Orthochirus glabrifrons*, (*O. afar*, *O.* 'innesi')))), or clade 3 = (*Fetilinia dentator*, (*Orthochirus glabrifrons*, (*O. afar*, *O.* 'innesi'))), or both, were resolved with significant support (jackknife statistic 50% – 71%) (Table 4, gray cells). This result was independent of reversibility of characters 1 and 2. Clades 2 and 3 excluded all species of *Orthochiroides*, and included *Orthochirus* and either one or both of two other genera, *Baloorthochirus* and *Fetilinia*. This implies that a group including only *Orthochiroides* and *Orthochirus* is polyphyletic, thereby refuting the proposed synonymy of these two genera. A genus including both *Orthochiroides* and *Orthochirus* would also need to include *Baloorthochirus* and *Fetilinia*, which have very different metasomal morphologies. Even then, it would require fusion of clades 1 and 2, which were not resolved as sister groups in any of our analyses. A monophyletic genus that includes both *Orthochirus* and *Orthochiroides* necessitates the inclusion the entire set of ingroup taxa (Figs. 205–209, 211).

A subset of our ingroup taxa was included in an extensive DNA analysis of buthid phylogeny (Štundlová et al., 2022). The relationships among these taxa reconstructed by Bayesian inference and maximum likelihood analysis applied to the entire buthid dataset are shown in Fig. 210. The species representing *Orthochiroides* occupied a basal position, separated from the lineages containing *Orthochirus* (shaded panels in Fig. 210). This separation, as well as the overall topology, were consistent our morphological analyses. Taken together, these findings further confirm the status of *Orthochiroides* as a genus separate from *Orthochirus*, as originally proposed by Kovařík (1998, 2004). The synonymy of *Orthochiroides* with *Orthochirus* by Lourenço & Ythier (2021) is hereby invalidated, and we reinstate *Orthochiroides* Kovařík, 1998 **stat. rev.**, with a differential diagnosis provided by the seven characters **(i) – (vii)**.

Off the nine different trees obtained in our analyses, the most frequent was T_0 (e.g., Fig. 205). It was retrieved repeatedly under equal weights and under implied weights with moderate to weak concavity constants. It also enjoyed the highest support values for clades 1, 2 and 3, and was our preferred phylogenetic hypothesis. Unambiguous synapomorphies for T_0 are mapped in Fig. 211.

Discussion

At first glance, the basal position of *Orthochiroides* relative to other ingroup taxa and its separation from *Orthochirus* revealed by cladistic analysis, may not be obvious. The general habitus, small size, dark coloration, trapezoidal carapace, abbreviated pedipalps, and stout metasomal segments with heavy sclerotization and specialized morphosculpture (pits or

depressions) on more posterior segments, all seem to suggest a closer relationship with *Orthochirus*. However, the weight of evidence from a larger set of characters analyzed collectively, as well as from wholly independent DNA analyses, imply that these similarities are superficial and are likely to have arisen by convergence. Small size and dark coloration are characters found in many other genera and families of scorpions. A trapezoidal carapace and abbreviated pedipalps are characters shared with most of the other ingroup genera of small buthids (*Neobuthus*, *Xenobuthus*, *Butheolus*, *Baloorthochirus* and *Fetilinia*). Moreover, the carapaces of *Orthochiroides* and *Orthochirus* occupy disjunct geometric domains in trapezoidal morphospace. The heavy sclerotization and specialized morphosculpture of metasomal segments in *Orthochiroides* and *Orthochirus* are not shared with other ingroup members, and could be synapomorphies relating the two genera. However, heavy sclerotization and punctate sculpture of the posterior metasoma, similar to that of *Orthochirus* spp., *Orthochiroides insularis* and *Orthochiroides socotrensis*, also occurs in the 'Buthus' group genus *Microbuthus* Kraepelin, 1898. Other characters, including uniquely modified pedipalps, imply that *Microbuthus* is more closely related to *Picobuthus* Lowe, 2010, a genus without punctate metasomal segments (Lowe, 2010). Indeed, DNA analysis placed *Microbuthus* and *Picobuthus* in a lineage separate from *Orthochiroides*, *Orthochirus* and the other ingroup taxa analyzed here (Štundlová et al., 2022). Other buthid genera with punctate posterior metasomal segments include *Butheoloides* Hirst, 1925, *Isometroides* Keyserling, 1885, *Karasbergia* Hewitt, 1913, and some species of *Uroplectes* (Hirst, 1925; Lourenço, 2001; Prendini, 2004, 2015). These all reside in clades external to the 'Buthus' group (Fet et al., 2005; Štundlová et al., 2022). The punctate metasoma admits a functional interpretation that can explain why it may be favored by parallel evolution and susceptible to homoplasy (Lowe, 2010). In buthids with weak pedipalps, the posterior metasoma combined with the telson function as the main offensive and defensive weapon, and is expected to be under selection pressure to develop thicker sclerotization. It may also have sensory functions (Fet et al., 2003), requiring deployment of sensillae over its cuticular surface. The punctae or pits simply represent foci where the exoskeleton is thinned to facilitate the connections of internal sensory neurons to external sensillae.

A character that we did not include in our diagnosis of *Orthochiroides* is the shape of the hemispermatophore basal lobe. Basal lobe shapes are potential diagnostic characters because they appear to be more or less conserved within many 'Buthus' group genera that have been studied (e. g., Kovařík et al., 2018). In *Orthochiroides somalilandus* **sp. n.**, the basal lobe is a broad hook with a triangular profile, projecting strongly out from the convex surface of the capsule (Figs. 46–48, 193–196). In several species of *Orthochirus* that we examined, the basal lobe is a 'laminate' hook that is more elongated with a lower profile (Figs. 197–204). Similar shapes of the basal lobe in *Orthochirus* have been recorded for a few species in the literature (Levy & Amitai, 1980: 99,

fig. 90; Vachon, 1952: 227, fig. 309). The hemispermatophore has not been described for other species of *Orthochiroides* and *Orthochirus*, and more studies are needed to determine if these differences can be generalized as diagnostic characters. In our data matrix, hook shapes of the other three species of *Orthochiroides*, and of *Baloorthochirus* and *Fetilinia* were scored as unknowns (?) and the character did not contribute much to the analysis. However, we note that a broad hook is also present in the outgroup genus *Compsobuthus* (Fig. 189). In *Neobuthus* and *Gint*, the basal lobe is also broad but the apical hook is less sharp (Figs. 190–192). *Orthochiroides* is more similar to these other genera in the form of its basal lobe, than to *Orthochirus*.

Under our preferred hypothesis, T_0, *Orthochiroides* is monophyletic, and its sister node is supported by six unique synapomorphies (Fig. 211). These involve coarsening of carapace granulation, attenuation and loss of carinae on the pedipalp and sternite VI, and development of glossy cuticle on sternite VI. At the next level of the tree, the branch leading to *Orthochirus* is supported by two synapomorphies (one unique). These both involve the carapace, i.e., a moderately trapezoidal shape, and loss of antero-submedian carinae. At the next bifurcation, clade 2 = (*Baloorthochirus*, (*Fetilinia*, *Orthochirus*)) diverges from its sister group containing *Butheolus* and *Xenobuthus*. Clade 2 is supported by six additional synapomorphies (3 unique). These involve loss of centromedian carinae on the carapace, loss of petite 'trichobothrium' d_2 on the dorsal femur, stepped widening of metasoma II–III posterior margins, and a telson with slender pyriform vesicle and shallow posterior slope. The metasoma and telson characters are unique to clade 2. Within clade 2, clade 3 contains *Fetilinia* and *Orthochirus* and is supported by four additional synapomorphies (one unique). These involve reduction of granule size on the carapace (a reversion from coarse to fine granulation), smoothening of pedipalp patella carinae, and the forward and outward extension of the anterior corners of metasoma III–IV. The latter character is unique, more weakly developed in *Fetilinia* (a partial or intermediate condition), and more strongly so in *Orthochirus*. We postulate an evolutionary sequence in which stepped widening of metasoma II–III posterior margins developed first in the ancestor of *Baloorthochirus*, followed by addition of a weak metasoma III–IV anterior corner flaring in the ancestor of *Fetilinia*. Finally, stronger anterior corner flaring in the ancestor of *Orthochirus* enabled a closer interlocking of successive metasomal segments, which is a unique structural adaptation of the genus which never evolved in *Orthochiroides*. The separation of clade 2 from *Orthochiroides* is supported by a total of 13 synapomorphies (10 unique), and the separation of clade 3 by a total of 17 synapomorphies (11 unique).

Under our preferred hypothesis, T_0, the pair of species of *Orthochiroides* endemic to Socotra Island (*O. insularis* and *O. socotrensis*) form a sister group with respect to the group composed of the pair of species found on the Horn of Africa mainland (*O. somalilandus* **sp**. **n**. and *O. vachoni*) (Fig. 211). The two sister groups are united under clade 1 by five

non-unique synapomorphies. These involve dark coloration, reduction of carinae on the carapace, development of a fringe of enlarged, sexually non-dimorphic denticles on the posterior margins of sternites III–V, and a bulbous telson. However, compared to the mainland species, the two Socotra species are more derived with five synapomorphies. These involve smoothening of pedipalp patella carinae, obsolescence of pedipalp chela manus E carina, proximal positioning of pedipalp fixed finger trichobothrium *dt* with respect to *et*, and a punctate metasoma II lateral surface. The punctate surface morphosculpture of the Socotra species extends over lateral and ventral metasoma III–V (Figs. 82–83), surfaces that are rugose-reticulate in the two mainland species (Figs. 13–14, 16–17, 84–85). The rugose-reticulate condition can be viewed as an intermediate stage of enhanced sclerotization of metasomal segments, in which the network of thickened wrinkles or ridges occupies less total surface area than the lacunae between them (Kovařík, 1998). In the Socotra species, the thickened exoskeleton has expanded to occupy a greater total surface area than the lacunae, which have contracted into smaller punctae or pits. Some of the most parsimonious trees retrieved under implied weights with strong concavity placed the Socotra species as a sister group of other ingroup genera (T_i, i = 3–5, 6, 8; e. g., Figs. 207–208). In these topologies *Orthochiroides* was paraphyletic. However, the sister relationship was supported by only two synapomorphies (weak E carina on pedipalp manus, loss of granulation on sternite V), whereas five synapomorphies supported monophyly of *Orthochiroides* with a sister relationship between the Socotra and the mainland African species (T_i, i = 0–2, 7, 9; e. g., Figs. 205–206, 209). We favor the latter hypothesis. We propose that the two species of *Orthochiroides* endemic to Socotra are descended from an old lineage that diverged from mainland *Orthochiroides* after a long period of isolation on the island. The length of the period depends on whether the split was by Gondwanan vicariance (38–34 Mya, or 20–17.6 Mya; Culek, 2013; Macey et al., 2008), or by more recent dispersal (e.g., 10–3 Mya; Sindaco et al., 2012). The two Socotra species could be placed in their own genus, although we prefer to await acquisition of molecular data that can estimate their time of divergence from the mainland lineage.

Comparative material examined

Baloorthochirus becvari Kovařík, 1996
Pakistan: SE Balochistan, Khurkhra, 38 km S of Uthal, 24.1V.I993, 1♂ (holotype) (FKCP), leg. S. Bečvář.

Butheolus gallagheri Vachon, 1980
Oman: main road above Khor Rori Beach, UV detection on ground, densely vegetated wadi, E of Taqah; warm and humid with many insects, 17°03.22'N 54°25.33'E, 50 m a. s. l., 18.X.1993, 21:24 h, 4♂11♀ (GLPC, NHMB, ONHM), leg. G. Lowe; Mirbat, 17°02.19'N 54°38.75'E, 54 m a. s. l., 4♂11♀ (FKCP).

Butheolus harrisoni Lowe, 2018
Oman: Jabal Qara; north slopes, Nejd, UV detection, rocky wadi & rocky slopes, 17°17.83'N 54°05.11'E, 800 m a. s. l., 16.X.1993, 22:38 h, 4♂7♀ (NHMB, USNM), leg. G. Lowe.

Butheolus thalassinus Simon, 1882
Yemen: Ta'izz, under rock on Euphorbia Aloe Hill, 3800 ft a. s. l., 10.I.1951, 1♂, (WDS), leg. H. Hoogstraal.

Compsobuthus eritreaensis Kovařík, Lowe, Plíšková & Šťáhlavský, 2016
Eritrea: near Massawa, 15°36'58.7"N 39°22'32.8"E, 74 m a. s. l., 4.-5.XI.2015 (Locality 15EI), 7♂12♀ (holotype and paratypes) (FKCP), ♂ hemispermatophore No. 877 (GLPC), leg. F. Kovařík.

Fetilinia dentator Lowe & Kovařík, 2021
Pakistan: Khyber Pakhtunkhwa (formerly North-Western Frontier) Province, Karak, 33.102°N 71.049°E, 23.VI.2010, 1♂ subadult (holotype) 1♀ juvenile (paratype) (FKCP), leg. Z. Ahmed.

Gint amoudensis Kovařík, Lowe, Just, Awale, Elmi & Šťáhlavský, 2018
Somaliland: Borama, Amoud University campus, 09°56'49"N 43°13'23"E, 1394 m a. s. l. (Locality No. 17SR =17SA), 9-13.IX.2017, 1♂ (holotype), 6♂3♀3♀juvs.2♂juvs. (FKCP), leg. F. Kovařík.

Gint banfasae Kovařík & Lowe, 2019
Somaliland: Shanshade vill., 08°39'35"N 45°55'49"E, 790 m a. s. l. (Locality No. 18SJ), 29–31.VIII.2018, 66♂8♀4juvs. (holotype and paratypes), Nos. 1530, 1531, 1532, 1533, 1534) (FKCP), 2♂ (GLPC). leg. F. Kovařík et al.

Gint maidensis Kovařík, Lowe, Just, Awale, Elmi & Šťáhlavský, 2018
Somaliland: Maid, 11°00'03"N 47°06'30"E, 52 m a. s. l. (Locality No. 17SN), 3.-4.IX.2017, 11♂9♀1im.♂1im.♀ (holotype, paratypes, Nos. 1321, 1324, 1336) (FKCP), ♂ hemispermatophores Nos. 1321, 1324, 1336 (GLPC), leg. F. Kovařík.

Neobuthus eritreaensis Lowe & Kovařík, 2016
Eritrea: near Massawa, 15°36'58.7"N 39°22'32.8"E, 74 m a. s. l., 4.XI.2015 (Locality No. 15EI), 1♂ (holotype) 4♀1♀im. (paratypes) (FKCP), 1♂1♀ (paratypes), ♂ hemispermatophore No. 877 (GLPC), leg. F. Kovařík.

Neobuthus kutcheri Lowe & Kovařík, 2016
Ethiopia: Somali State, Liben region, Filtu, 05°06'48.7"N 40°39'18.3"E, 1229 m a. s. l., (Locality No. 14EG), 19.-21.XI.2014, 4♂ (holotype and paratypes) 6♀5♀ims.7juvs. (paratypes) (FKCP), 2♂3♀3♀ims.2juvs. (paratypes) (GLPC), leg. F. Kovařík et al.

Orthochirus afar Kovařík & Lowe, 2016
Ethiopia: Afar Region, Gewane, 10°09'38"N 40°39'45"E, 631 m a. s. l. (Locality No. 12EO), 23–24.XI.2012, 1♂ holotype, 1♂1♀ paratypes, 1♂juv. paratype (FKCP), leg. F. Kovařík; 11°43'22"N 40°56'52"E, 457 m a. s. l. (Locality No. 12EM), 20.XI.2012, 1♀juv. (paratype) (FKCP), leg. F. Kovařík.
Somaliland: Gerissa, N of Borama, 10°36'01"N 43°26'07"E, 245 m a. s. l. (Locality No. 17ST), 11.-12.IX.2017 (FKCP), ♂ hemispermatophores No. 1301, 1328 (GLPC), leg. F. Kovařík.

Orthochirus glabrifrons (Kraepelin, 1903)
Oman: Dibab, woodland behind beach, 23°06'N 59°02'E (Locality No. 1991013101) 31.I.1991, 3♂2♀1im. (GLPC), leg. A. S. Gardner; Wadi Bani Kharus, 23°11.32'N 57°34.77'E, 800 m a. s. l. (Locality No. 1992101105), 11.X.1993, 6♂1♀ (FKCP, GLPC), leg. G. Lowe, A. S. Gardner, S. M. Farook; Jabal Bani Jabir, 22.813172°N 59.058884°E, 2017, ♂ hemispermatophore No. 1389 (GLPC), leg. M. Stockmann.

Orthochirus cf. '*glabrifrons*' (Kraepelin, 1903)
Oman: W of Wadi Andhur, 17.6877488°N 54.5917380°E, X.2019, 1♂1♀, ♂ hemispermatophore No. 1389 (GLPC), leg. M. Stockmann; Kawdaki, ♂ hemispermatophore No. 1219 (GLPC).

Orthochirus cf. '*innesi*' Simon, 1910
Oman: Batinah plain, 10–15 km W of Barka, Abyad pipeline, coastal dunes, edge of *Acacia* woodland, 23°41.16'N 57°43.61'E, 50 m a. s. l. (Locality No. 1993101302), 13.X.1993, 2♂1♀ (GLPC), leg. G. Lowe, A. S. Gardner, S. M. Farook; E of Thumrait, road to Marmul, wide gravel wadi, 17°39.62'N 54°9.11'E, 500 m a. s. l. (Locality No. 1993101901), 19.X.1993, 3♂1♀ (NHMB), leg. G. Lowe; Wadi Halfayn, E. of Adam, 22°26.81'N 57°39.36'E, 290 m a. s. l. (Locality No. 1995091603), 16.IX.1995, 3♂ (NHMB), leg. G. Lowe, J. Dundon; E of Thumrait, wide, soft sandy wadi, 17°42'N 53°59'E (Locality No. 1997020002), 12.II.1997, 8.-11.III.1997 3♂3♀1im. (NHMB, ONHM), leg. G. Lowe, J. Dundon; Wadi Rawnab, 18.82781°N 56.40250°E, 2017, 2♂ hemispermatophores No. 1390, 1391 (GLPC), leg. M. Stockmann.

Orthochirus scrobiculosus (Grube, 1873)
Turkmenistan: Balkan Province, Krasnovodsk [now Türkmensbashi, 40.02°N 52.97°E], 1♀ lectotype, leg. Dr. [Gustav] Radde, [June 1870], MNHW No. 531.

Orthochirus sp.
Morocco: 28.51619°N 09.85365°W, X.2016, 7♂ (No. 16F81), ♂ hemispermatophore No. 1164 (GLPC), leg. M. Stockmann; N. of Msied, 28.09221°N 10.88881°W, X.2016, 1♂2♀ (No. 16F83), ♂ hemispermatophores No. 1165–1168 (GLPC), leg. M. Stockmann.

Somalibuthus sabae Kovařík & Njoroge, 2021.
Kenya: Kiwayu Island, Lamu County, 1°59'36.32"S 41°17'08.59"E, 14.XII.2020, 1♂ (holotype, NMK/ INV/T-238), 2♂4♀ (paratypes, NMK/INV/T-239-244), leg. S. Douglas-Hamilton.

Xenobuthus anthracinus (Pocock, 1895)
Oman: S of Thumrait, Nejd Desert, UV detection, edge of small vegetated wadi, open plain, fine silty soil, rock outcrops, 17°30.76'N 54°02.76'E, 580 m a. s. l., 16.X.1993, 19:28 h, 1♀, leg. G. Lowe, (NHMB); S of Thumrait; Nejd Desert, UV detection, silty plain, edge of small vegetated wadi, fine silty soil, open plain, rock outcrops, 17°30.77'N 54°02.82'E, 600 m a. s. l., 19.X.1993, 23:02 h, 1♂, leg. G. Lowe, (NHMB).

Xenobuthus xanthus Lowe, 2018
Oman: Jabal Zulul, escarpment above Ash Shuwaymiyah, UV detection on ground, silt and gravel, rocky bowl surrounded by rocky cliffs and slopes, 17°57.12'N 55°39.28'E, 215 m a. s. l., 1♂ (holotype), 26.IX.1995, leg. G. Lowe, M. D. Gallagher (NHMB); Wadi Ara, Jabal Samhan, under rocks at base of cliff, 17°16'N 54°57'E, 1050 m a. s. l., 2.II.1994, 1♀, leg. M. R. Brown (ONHM); Wadi Shuwaymiyah, under rock on mound of sandy soil, near permanent water seepage site on northern edge of wide vegetated wadi, 17°55.94'N 55°31.47'E, 50 m a. s. l., 25.IX.1995, 19:15 h, 1♀, leg. G. Lowe, M. D. Gallagher (NHMB).

Acknowledgements

References

ACOSTA, L. E., D. M. CANDIDO, E. H. BUCKUP & A. D. BRESCOVIT. 2008. Description of *Zabius gaucho* (Scorpiones, Buthidae), a new species from southern Brazil, with an update about the generic diagnosis. *Journal of Arachnology*, 36: 491–501.

BIRULA, A. A. 1917. Chlenistobryukhie paukoobraznye Kavkazskogo Kraya. Part I. Scorpiones. *Zapiski Kavkazskogo Muzeya*, 5: 1–253.

CHEUNG, C., L. DE VANTIER & K. VAN DAMME. 2006. *Socotra. A Natural History of the Islands and Their People*. Odyssey.

CULEK, M. 2013. Geological and morphological evolution of the Socotra Archipelago (Yemen) from the biogeographical view. *Journal of Landscape Ecology*, 6 (3):84–108.

DUPRÉ, G. 2007. Conspectus genericus scorpionorum 1758–2006 (Arachnida: Scorpiones). *Euscorpius*, 50: 1–31.

EL-HENNAWY, H. K. 1992. A catalogue of the scorpions described from the Arab countries (1758-1990) (Arachnida: Scorpionida). *Serket*, 2(4): 95–153.

FET, E. V., D. NEFF, M. R. GRAHAM & V. FET. 2003. Metasoma of *Orthochirus* (Scorpiones: Buthidae): are scorpions evolving a new sensory organ? *Revista Ibérica de Aracnología*, 8: 69–72.

FET, V. & F. KOVAŘÍK. 2020. New scorpion taxa (Arachnida: Scorpiones) described in the journal "Euscorpius" in 2002–2020. *Euscorpius*, 300: 1–31.

FET, V. & G. LOWE. 2000. *Family Buthidae C. L. Koch, 1837*, pp. 54–286 in: Fet, V., Sissom, W. D., G. Lowe & M. E. Braunwalder. 2000. *Catalog of the Scorpions of the World* (*1758-1998*). The New York Entomological Society, New York, 689 pp.

FET, V. & M. E. SOLEGLAD. 2005. Contributions to Scorpion Systematics. I. On Recent Changes in High-Level Taxonomy. *Euscorpius*, 31: 1–13.

FET, V., M. E. SOLEGLAD & G. LOWE. 2005. A new trichobothrial character for the high-level systematics of Buthoidea (Scorpiones: Buthida). *Euscorpius*, 23: 1–40.

FRANCKE, O. F. 1977. Taxonomic observations on *Heteronebo* Pocock (Scorpionida: Diplocentridae). *Journal of Arachnology*, 4: 95–113.

GOLOBOFF, P. A. 1993. Estimating character weights during tree search. *Cladistics*, 9: 83–91.

GOLOBOFF, P. A., J. S. FARRIS, M. KÄLLERSJÖ, B. OXELMAN, M. J. RAMÍREZ & C. A. SZUMIK. 1993. Improvements to resampling measures of group support. *Cladistics*, 19: 324–332.

GOLOBOFF, P. A. & S. A. CATALANO. 2016. TNT version 1.5, including a full implementation of phylogenetic morphometrics. *Cladistics*, 32: 221–238.

HIRST, S. 1925. On some scorpions from Morocco, with the description of a new genus and species. *Annals and Magazine of Natural History*, 9 (15): 414–416.

HŮLA, V. & J. NIEDOBOVÁ. 2020. The Mediterranean Recluse Spider *Loxosceles rufescens* (Dufour, 1820): a new invasive for Socotra Island (Yemen). *Rendiconti Lincei. Scienze Fisiche e Naturali*, https://doi.org/10.1007/s12210-020-00925-7.

KARSCH, F. 1891. Arachniden von Ceylon und von Minikoy gesammelt von den Herren Doctoren P. und S. Sarasin. *Berliner Entomologische Zeitschrift*, 36 (2): 267–310.

KOVAŘÍK, F. 1996. *Baloorthochirus becvari* gen. et sp. n. from Pakistan, and taxonomic position of *Orthochirus luteipes* (Scorpiones: Buthidae). *Acta Societatis Zoologicae Bohemoslovenicae*, 60: 177–181.

KOVAŘÍK, F. 1998. Three new genera and species of Scorpiones (Buthidae) from Somalia. *Acta Societatis Zoologicae Bohemicae*, 62: 115–124.

KOVAŘÍK, F. 2000. The Socotra Island and its scorpions. *Akvárium terárium*, 43(7): 63–67 (in Czech).

KOVAŘÍK, F. 2002. A checklist of scorpions (Arachnida) in the collection of the Forschungsinstitut und Naturmuseum Senckenberg, Frankfurt am Main, Germany. *Serket*, 8(1): 1–23.

KOVAŘÍK, F. 2003. Scorpions of Djibouti, Eritrea, Ethiopia, and Somalia (Arachnida: Scorpiones), with a key and descriptions of three new species. *Acta Societatis Zoologicae Bohemicae*, 67: 133–159.

KOVAŘÍK, F. 2004. Revision and taxonomic position of genera *Afghanorthochirus* Lourenço & Vachon, *Baloorthochirus* Kovařík, *Butheolus* Simon, *Nanobuthus* Pocock, *Orthochiroides* Kovařík, *Pakistanorthochirus* Lourenço, and Asian *Orthochirus* Karsch, with descriptions of twelve new species (Scorpiones, Buthidae). *Euscorpius*, 16: 1–33.

KOVAŘÍK, F. 2009. *Illustrated catalog of scorpions. Part I.* Jakub Rolčík – Clairon Production, Prague, 170 pp.

KOVAŘÍK, F., V. FET & M. SIYAM. 2020a. Taxonomic position of *Orthochirus olivaceus* (Karsch, 1881),the type species of the genus *Orthochirus* Karsch, 1892 (Scorpiones: Buthidae). *Euscorpius*, 319: 1–15.

KOVAŘÍK, F., V. FET & E. A YAĞMUR. 2020b. Further review of *Orthochirus* Karsch, 1892 (Scorpiones: Buthidae) from Asia: taxonomic position of *O. melanurus*, *O. persa*, *O. scrobiculosus*, and description of six new species. *Euscorpius*, 318: 1–73.

KOVAŘÍK, F. & G. LOWE. 2012. Review of the genus *Neobuthus* Hirst, 1911 with description of a new species from Ethiopia (Scorpiones: Buthidae). *Euscorpius*, 138: 1–25.

KOVAŘÍK, F. & G. LOWE. 2019. Scorpions of the Horn of Africa (Arachnida, Scorpiones). Part XVIII. *Gint banfasae* sp. n. from Somaliland (Buthidae). *Euscorpius*, 2729: 1–14.

KOVAŘÍK, F. & G. LOWE. 2020. Scorpions of the Horn of Africa (Arachnida: Scorpiones). Part XXIV. *Leiurus* (Buthidae), with description of *Leiurus gubanensis* sp. n. *Euscorpius*, 309: 1–19.

KOVAŘÍK, F. & G. LOWE. 2021. Scorpions of the Horn of Africa (Arachnida: Scorpiones). Part XXVI. Records of *Hottentotta polystictus* (Pocock, 1896), with descriptions of *H. haudensis* sp. n. and *H. nigrimontanus* sp. n. (Buthidae) from Somaliland. *Euscorpius*, 330: 1–28.

KOVAŘÍK F., G. LOWE, P. JUST, A. I. AWALE, H. SH A. ELMI & F. ŠŤÁHLAVSKÝ. 2018. Scorpions of the Horn of Africa (Arachnida: Scorpiones). Part XV. Review of the genus *Gint* Kovařík et al., 2013, with description of three new species from Somaliland (Scorpiones, Buthidae). *Euscorpius*, 259: 1–41.

KOVAŘÍK, F., G. LOWE, J. PLÍŠKOVÁ & F. ŠŤÁHLAVSKÝ. 2013. A new scorpion genus, *Gint* gen. n., from the Horn of Africa (Scorpiones: Buthidae). *Euscorpius*, 138: 1–19.

KOVAŘÍK, F., G. LOWE, J. PLÍŠKOVÁ & F. ŠŤÁHLAVSKÝ. 2016b. Scorpions of the Horn of Africa (Arachnida: Scorpiones). Part VI. *Compsobuthus* Vachon, 1949 (Buthidae), with a description of *C. eritreaensis* sp. n.. *Euscorpius*, 226: 1–21.

KOVAŘÍK, F., G. LOWE & F. ŠŤÁHLAVSKÝ. 2016a. Scorpions of the Horn of Africa (Arachnida: Scorpiones). Part IX. *Lanzatus*, *Orthochirus*, and *Somalicharmus* (Buthidae), with description of *Lanzatus somalilandus* sp. n. and *Orthochirus afar* sp. n. *Euscorpius*, 232: 1–38.

KOVAŘÍK, F. & S. NAVIDPOUR. 2020. Six new species of *Orthochirus* Karsch, 1892 from Iran (Scorpiones: Buthidae). *Euscorpius*, 312: 1–41.

KOVAŘÍK, F. & A. A. OJANGUREN AFFILASTRO. 2013. *Illustrated catalog of scorpions. Part II. Bothriuridae*; *Chaerilidae*; *Buthidae I. Genera* Compsobuthus, Hottentotta, Isometrus, Lychas *and* Sassanidotus. Prague: Clairon Production, 400 pp.

KOVAŘÍK, F. G. LOWE & T. MAZUCH. 2019a. Scorpions of the Horn of Africa (Arachnida: Scorpiones). Part XIX. *Pandiborellius meidensis* (Karsch, 1879) and *Pandinurus fulvipes* sp. n. (Scorpionidae) from Somaliland. *Euscorpius*, 275: 1–18.

KOVAŘÍK, F., E. A YAĞMUR, V. FET & F. S. HUSSEN. 2019b. A review of *Orthochirus* from Turkey, Iraq, and Iran (Khoozestan, Ilam, and Lorestan Provinces), with descriptions of three new species (Scorpiones: Buthidae). *Euscorpius*, 278: 1–31.

KRAEPELIN, K. 1903. Scorpione und Solifugen Nordost-Afrikas, gesammelt 1900 und 1901 von Carlo Freiherrn von Erlanger und Oscar Neumann. *Zoologische Jahrbücher, Abtheilung für Systematik*, 18 (4-5): 557–578.

LEVY, G. & P. AMITAI. 1980. Scorpiones. Fauna Palaestina. Arachnida I. *The Israel Academy of Sciences and Humanities*. Jerusalem 1980.

LORIA, S. F. & L. PRENDINI. 2014. Homology of the lateral eyes of Scorpiones: a six-ocellus model. *PLoS ONE* 9(12): e112913. doi:10.1371/journal.pone.0112913

LOURENÇO, W. R., 2001. Taxonomic considerations on the genera *Butheolus* Simon, *Nanobuthus* Pocock and *Neobuthus* Hirst (Scorpiones, Buthidae) with the description of a new species of *Neobuthus* from Ethiopia. Pp. 171-183 in I. Prakash (ed.) Ecology of desert environments. Scientific Publishers (India), Jodhpur.

LOURENÇO, W. R. 2006. Nouvelle proposition de découpage sous-générique du genre *Tityus* C. L. Koch, 1836 (Scorpiones, Buthidae). *Boletín Sociedad Entomológica Aragonesa*, 39: 55–67.

LOURENÇO W. R. & YTHIER E. 2021. A particular new species of *Orthochirus* Karsch, 1891 from Somalia (Scorpiones: Buthidae). *Serket*, 17 (4): 335–349.

LOWE, G. 2010. New picobuthoid scorpions (Scorpiones: Buthidae) from Oman. *Euscorpius*, 93: 1–53.

LOWE, G. 2018. The genera *Butheolus* Simon, 1882 and *Xenobuthus* gen. nov. (Scorpiones: Buthidae) in Oman. *Euscorpius*, 261: 1–73.

LOWE, G. & F. KOVAŘÍK. 2016. Scorpions of the Horn of Africa (Arachnida, Scorpiones). Part V. Two new species of *Neobuthus* Hirst, 1911 (Buthidae), from Ethiopia and Eritrea. *Euscorpius*, 224: 1–46.

LOWE, G. & F. KOVAŘÍK. 2021. *Fetilinia dentator* gen. et sp. n. from Pakistan (Scorpiones: Buthidae). *Euscorpius*, 328: 1–10.

LOWE, G., E. A. YAĞMUR & F. KOVAŘÍK. 2014. A review of the genus *Leiurus* Ehrenberg, 1828 (Scorpiones: Buthidae) with description of four new species from the Arabian Peninsula. *Euscorpius*, 191: 1–129.

LOWE, G., F. KOVAŘÍK, M. STOCKMANN & F. ŠŤÁHLAVSKÝ. 2019. *Trypanothacus* gen. n., a new genus of burrowing scorpion from the Arabian Peninsula (Scorpiones: Buthidae). *Euscorpius*, 277: 1–30.

LEVY, G. & P. AMITAI. 1980. *Fauna Palaestina, Arachnida I.– Scorpiones*. The Israel Academy of Sciences and Humanities, 132 pp.

MACEY, J. R., J. V. KUEHL, A. LARSON, M. D. ROBINSON, I. H. UGURTAS, N. B. ANANJEVA, H. RAHMAN, H. I. JAVED, R. M. OSMAN, A. DOUMMAK & T. J. PAPENFUSS. 2008. Socotra Island the forgotten fragment of Gondwana: Unmasking chameleon lizard history with complete mitochondrial genomic data. *Molecular Phylogenetics and Evolution*, 49: 1015–1018

NAVIDPOUR, S., F. KOVAŘÍK, M. E. SOLEGLAD & V. FET. 2019. Scorpions of Iran (Arachnida, Scorpiones). Part X. Alborz, Markazi and Tehran Provinces with a description of *Orthochirus carinatus* sp. n. (Buthidae). *Euscorpius*, 276: 1–20.

POCOCK, R. I. 1889. Notes on some Buthidae, new and old. *Annals and Magazine of Natural History*, 3: 334– 351.

POCOCK, R. I. 1899. The expedition to Socotra. III. Descriptions of the new species of scorpions, centipedes, and millipedes. *Bulletin of the Liverpool Museums*, 2: 7–9.

POCOCK, R. I. 1903. The Scorpions and Spiders of Sokotra. Pp.178–182 In Forbes H. O.: *The natural History of Sokotra and Abd-el-Kuri* (*Special Bulletin of the Liverpool Museums*). Henry Young and Sons, Liverpool.

PRENDINI, L. 2004. Revision of *Karasbergia* Hewitt (Scorpiones; Buthidae), a monotypic genus endemic to southern Africa. *Journal of Afrotropical Zoology*, 1: 77– 93.

PRENDINI, L. & W. WHEELER. 2005. Scorpion higher phylogeny and classification, taxonomic anarchy, and standards for peer review in online publishing. *Cladistics*, 21: 446–494.

PRENDINI, L. 2015. Three new *Uroplectes* (Scorpiones: Buthidae) with punctate metasomal segments from tropical central Africa. *American Museum Novitates*, 3840: 1–32.

PURCHART, L., V. HŮLA & Z. F. FRIČ. 2020. Comparison of the biogeographic origin of three terrestrial arthropod groups in the Socotra Archipelago (Yemen). *Rendiconti Lincei. Scienze Fisiche e Naturali*, 31: 623–635.

RASBAND, W. S. 1997–2018. ImageJ, U.S. National Institutes of Health, Bethesda, Maryland, USA, http://imagej.nih.gov/ij/.

REIN, J. O. 2022. The Scorpion Files. https://www.ntnu.no/ub/scorpion-files/ (accessed 1.III.2022)

SENAN, A. S., R. K. SOMASHEKAR, F. ATTORRE, N. TALEB & F. BRUNO. 2010. Exotic species of Socotra Island, Yemen: a first contribution. *Annali di Botanica*, https://doi.org/10.4462/annbotrm-9115

STAHNKE, H. L. 1971. Scorpion nomenclature and mensuration. *Entomological News*, 81(12): 297–316.

SIMON, E. 1910. Révision des Scorpions d'Égypte. *Bulletin de la Sociètè Entomologique d'Égypte*, 1910: 57–87.

SINDACO, R., M. METALLINOU, F. PUPIN, M. FASOLA & S. CARRANZA. 2012. Forgotten in the ocean: systematics, biogeography and evolution of the *Trachylepis* skinks of the Socotra Archipelago. *Zoologica Scripta*, 41: 346–362.

SISSOM, W. D. 1990. Systematics, biogeography and paleontology. Pp. 64–160 in POLIS, G. A. (Ed.) *The Biology of Scorpions*. Stanford University Press, Stanford, California.

SISSOM, W. D., G. A. POLIS & D. D. WATT. 1990. Field and laboratory methods. Pp. 445–461 in POLIS, G.A. (ed.). *The Biology of Scorpions*. Stanford University Press, Stanford, CA.

STAHNKE, H. L. 1972. A key to the genera of Buthidae (Scorpionida). *Entomological News*, 83 (5): 121–133.

ŠTUNDLOVÁ, J., F. ŠŤÁHLAVSKÝ, V. OPATOVÁ, J. ŠTUNDL, F. KOVAŘÍK, P. DOLEJŠ & J. ŠMÍD. 2022. Molecular data do not support the traditional morphology-based groupings in the scorpion family Buthidae (Arachnida: Scorpiones). *Molecular Phylogenetics and Evolution* (in press).

VACHON, M. 1952. Études sur les scorpions. *Institut Pasteur d'Algérie, Alger*, 1–482. (published 1948–1951 in *Archives de l'Institut Pasteur d'Algérie*, 1948, 26: 25–90, 162–208, 288–316, 441–481. 1949, 27: 66–100, 134–169, 281–288, 334–396. 1950, 28: 152–216, 383–413. 1951, 29: 46–104).

VACHON, M. 1963. De l`utilité, en systématique d`une nomenclature des dents des chelicéres chez les scorpions. *Bulletin du Muséum National d'Histoire Naturelle Paris*, 35(2): 161–166.

VACHON, M. 1974. Étude des caractères utilisés pour classer les familles et les genres de Scorpions (Arachnides). 1. La trichobothriotaxie en Arachnologie, Sigles trichobothriaux et types de trichobothriotaxie chez les Scorpions. *Bulletin du Muséum National d'Histoire Naturelle Paris*, 140: 857–958.

VACHON, M. 1975. Sur l'utilisation de la trichobothriotaxie du bras des pédipalpes des Scorpions (Arachnides) dans le classement des genres de la famille des Buthidae Simon. *Comptes Rendus Hebdomadaires des Séances de l'Académie des Sciences*, *Paris*, sér. D, 281: 1597–1599.

VOLSCHENK, E. S., G. T. SMITH & M. S. HARVEY. 2000. A new species of *Urodacus* from Western Australia, with additional descriptive notes for *Urodacus megamastigus* (Scorpiones). *Records of the Western Australian Museum*, 20 (1): 57–67.

WITT, A., V. HŮLA, A. S. S. SULEIMAN, K. VAN DAMME. 2020. First record of the red palm weevil *Rhynchophorus ferrugineus* (Olivier) on Socotra Island (Yemen), an exotic pest with high potential for adverse economic impacts. *Rendiconti Lincei. Scienze Fisiche e Naturali*, https://doi.org/10.1007/s12210-020-00918-6

YANG, X., Y. NORMA-RASHID, W. R. LOURENÇO & M. ZHU. 2013. True lateral eye numbers for extant buthids: a new discovery on an old character. *PLoS ONE*, 8(1): e55125. doi:10.1371/journal.pone.0055125.